RESPONSES to REFEREE #1

The paper summarizes results on optical properties of aerosols generated by burning of 3 common fuels in Africa. Some measurements were carried out on fresh BBOA, some on BBOA aged in the dark, some on photooxidized BBOA in the presence or absence of additional VOCs (typical urban aromatics). Fuels were burned at low (500 C) and high (800 C) temperatures. Non-refractory chemical composition of the aerosol was also measured, although not really discussed here. Single scattering albedo data, determined on size-selected aerosols, at mid-visible confirmed production of more absorbing aerosols under high temperatures. There was not a strong wavelength dependence to SSA between 500-570 nm. Dark aging of the BBOA resulted in increase in SSA possibly due to condensation of SOA and increase in the scattering cross section. The novelty of the experiment is in the selection of the fuels. However, I see some flaws in the approach (contribution of multiply charged particles was not corrected for in Mie calculations); the paper does not seem complete without the description of the compositional measurements (some conclusions are drawn on the composition of SOA without providing any support; there were no measurements of BC, yet overall refractive indices were estimated to use in Mie calculations); last the chamber oxidation experiments in the presence of additional VOCs don't seem to have worked. There were also several sentences that were confusing and need to be rephrased/clarified. Overall, I don't find the quality of this paper appropriate for ACP and cannot support any revisions.

AUTHORS RESPONSE: *We thank the reviewer for valuable and helpful suggestions. Embarrassing grammatical errors and sentences that seemed confusing will be corrected in the revision and changes made to the manuscript are provided here. Detailed responses are provided on the scientific questions raised. The authors feel that the reviewer either misunderstood our descriptions and overlooked some aspects of the paper. We will show this is indeed true in our detailed responses with relevant references to each question and comment. We feel that there is rush to dismiss and devalue the work and undermine the paper instead of giving us a chance to respond and clarify our claims. We hope our responses and explanations will convince the referee to make a different final determination.*

Three main issues raised by the reviewer in his/her the first paragraph is discussed below:

A. **"Non-refractory chemical composition of the aerosol was also measured, although not really discussed here"**

We would like to point out to the reviewer that this work is presented and submitted as a two-part paper, where part 1 was focused on optical properties and part II focused on chemical composition and characterization published in ACPD (Smith et al., 2020). Further integration of the two manuscripts will be done, and summaries from Part 2 will be incorporated into the revised manuscript. Following the paragraph contrasting eucalyptus and acacia combusted at 800^{o} C, the following text will be added to line 393:

"In the companion paper to this (Part 2), methanol extracts from BBA collected on Teflon filters were analyzed by ultra-performance liquid chromatography interfaced to both a diode array detector and an electrospray ionization high-resolution quadrupole time-of-flight mass spectrometer (UPLC/DAD-ESI-HR-QTOFMS) in negative ion mode. This was used to determine

the relative abundance and light-absorption properties of biomass burning organic aerosol constituents. MS analysis of BBA extracts from combustion at 800 °C revealed very little difference between the two fuel types, suggesting that there are either very few BrC species produced for either fuel under these combustion conditions, or there are numerous species that are essentially the same between the samples. However, given that Eucalyptus has a higher SSA than Acacia, this would suggest that Eucalyptus has more non-absorbing OA, or at least less absorbing than BC. Since it is Acacia that appears to have many more low-abundant organic constituents, several possibilities exist to explain these differences in SSA, as explored in more depth in Part 2. It is likely that Eucalyptus combustion products are not captured by some aspect of the extraction and UPLC/DAD-ESI-HR-QTOFMS analyses, that the observed differences in SSA are due to morphology differences, or some combination thereof. One potential explanation would be the presence of significant amounts of eucalyptol in the BBA, which is a large fraction of Eucalyptus oil, and is a cyclic ether that lacks any basic functionality amiable for negative ion mode analysis, has good solubility in alcohols, and does not absorb in the UV and visible. An examination of the UV-Visible spectra from the DAD shows no absorbing species in either region."

The following paragraph will be included in manuscript following the discussion of fresh emissions produced by combusted at 500^{o} C, added to line 410:

"Chemical analysis revealed that, when combusted at 500 °C, eucalyptus and acacia had a variety of compounds in common, such as lignin pyrolysis products, distillation products, and cellulose breakdown products. Several lignin pyrolysis products and distillation products are more prevalent in Eucalyptus than Acacia, while pyrolysis products of cellulose and at least one nitroaromatic species were more prevalent in Acacia. Given that these lignin pyrolysis and distillation products are known chromophores and are more prevalent in Eucalyptus than Acacia, while Acacia has a higher abundance of non-chromophores derived from sugars and cellulose, one would assume that Eucalyptus would be more absorbing in the visible (i.e. have a lower SSA) than Acacia. Despite the chemical analysis not capturing absolute amounts of OA, Acacia was found to have an SSA that is higher than Eucalyptus by 0.1 to 0.2, which is consistent with chemical measurements. This suggests that Acacia has either larger absolute amounts of non-chromophore compounds or Eucalyptus has a greater quantity of chromophores whose absorptive properties extend to the 500 – 570 nm region of the visible spectrum. An analysis of the chromatographically-integrated UV/Visible spectrum shows that there are chromophores whose absorption features peak ~290 nm and extend into the 500 – 570 nm region, though a normalized spectrum does not appear to show drastic differences between species."

Later, starting at line 504 with the sentence "We attempted…", the remainder of this paragraph and the next (after Figure 7) will be replaced with the following text:

"Despite the use of anthropogenic VOCs a concentrations larger than those average values found in urban and suburban regions of South Africa, no distinct effect was observed for SSA values of BBA produced during combustion at 500 °C. While it is possible that the relatively long aging time could obscure some of the effects due to the presence of VOCs, it is also possible that combustion products dominate molecular species and the effects of additional VOCs are insignificant. The later would suggest that anthropogenic pollution does not seem to affect the optical properties of BBA. Indeed, in examining the effects of aging on the chemical composition

of BBA shows very few species that could be attributed to anthropogenic VOCs; specifically, only dihydroxyphthalic acid produced from xylene. For both Eucalyptus and Acacia, an isomer of dihydroxybenzene, such as resorcinol or catechol, was removed to the highest degree from the fresh BB aerosol upon photochemical aging. Generally, very few compounds were produced to a significant extent and both fuels were dominated by loss of chromatophoric lignin pyrolysis and distillation products. Not surprisingly, the associated absorbance from these chromophores, mostly from 200 – 350 nm, also attenuated with respect to age. This may be caused in part by the photo-bleaching effect created by irradiation of UV light for 12 hours, heterogeneous OH oxidation, and SOA formation of non-chromophores.

This fact suggests that a study with a higher temporal resolution is needed to simulate the impact of the VOCs on aerosol SSA, where continuous or much more frequent measurement are needed to determine impact of urban pollution on aerosol single scattering albedo. Such a study, using continuous measurements, is not possible for our setup when particles are also size selected. Like dark aged conditions, we were not able to estimate SSA for combustion at 800 ^{o}C due to the low particle concentration and highly absorbing nature of the aerosol. A chemical analysis of aged BBA produced at this temperature revealed very few changes, suggesting there are few molecular species produced by combustion at this temperature."

B. **"However, I see some flaws in the approach (contribution of multiply charged particles was not corrected for in Mie calculations***"*

*There seems to be a misunderstanding regarding Mie calculation. As stated on P 11, L 356-358, we estimated the SSA of size-selected aerosol using the refractive indices estimated by Bond and Bergstrom, (2006) and Levin et al. (2010) for BC and bulk aerosol. The whole purpose of this effort was to explore if our estimated SSA for 200 nm size particles was impacted by the presence of multiply charge particles. The impact of multiply charged particles on SSA for 300 and 400 nm size particles was minimal. We only run the Mie models to make a qualitative comparison of Mie result with our measurements, focusing on the SSA dependence on particle size. The disclaimer "*Neither line is a fit to the data.*" Will be added to the caption of Figure 3. Further discussion on multiply charged particles is provided below in response to reviewer comments on* L361-362.

C. **"Some conclusions are drawn on the composition of SOA without providing any suppor**t"

The focus of the work is not SOA formation. However, as we observe changes in SSA we looked at the data more closely as stated on P 16, Line 460, we hypothesized that there could be SOA production during dark aging, and we cited previous work showing nitrogen-containing SOA production under nighttime conditions as potential chemical basis for this observation. As clearly stated in our discussion and in the abstract section, we hypothesized SOA production during dark aging but never definitively concluded about composition of SOA, as we do not have measurements for these experiments. We were inferring to work that was previously reported and focused on SOA formation during dark aging. (Tiitta et al., 2016;Li et al., 2015;Hartikainen et al., 2018). It seems that our statement regarding this was misunderstood and needs further clarification, which will be included in the revised draft.

Furthermore, the statement "there were no measurements of BC, yet overall refractive indices were estimated to use in Mie calculations" is not valid in our work given we never stated that we estimated refractive indices nor do we present any refractive indices of our own at any point. We have provided more details about this in response to the comment on L357.

The reviewer is mischaracterizing things as "additional VOCs don't seem to have worked". Just because something didn't significantly change, doesn't mean it didn't work. It just means that it doesn't seem to have had an impact.

Other specific comments are listed below: -
L 20-21: Bad grammar –
Agreed. *It will now read as "This work represents the first such study of the optical and chemical properties of three wood fuel samples used commonly for domestic use in east Africa."*
L 23-24: bad grammar –
Agreed: *"values are in the range between 0.287 and 0.439 while the SSA for fuels combusted at 500^{o} C, the range is between 0.66 and 0.769"*
L32: "injecting" and not "ejecting" –
Agreed: *ejecting will be replaced by injecting*
L33: it's unclear why measurements after 12 hrs. of injecting VOCs and BB aerosol in the chamber were not useful. –
We believe that measurements should have been made soon after injecting the VOC's
L 43: "measuring the. . ." –
"of" will be removed
L47: "partial evaporation. . ." –
Agreed: *partial evolution should be partial evaporation*
L85: "authors'. . ." –
Will be replaced with "To our knowledge"

L112: The sentence related to drying of the fuels should be moved earlier, before the weighing discussion. –

***AUTHORS RESPONSE**: We agree with the reviewer. Sentence related to drying of the fuels will be moved earlier, before the weighing discussion.*

L115: the EF mentioned is for tropical forests, which is not really representative of the African fuel's studies here. Please provide your justification for using this value. –

***AUTHORS RESPONSE**: We agree with the reviewer. We will delete the whole sentence talking about the EF and will add the following text:*

"During all the experiments, we normally burned 0.5 grams of fuel which produced about 600 to 800 µg m^{-3} of mass loading in the chamber. The mass loading was estimated by determining the total aerosol volume, based on measuring the volume distribution with an SMPS and assuming a density of 1 g cm^{-3} for fresh aerosol."

L164-165: It's unclear what is meant here "SSA and AAE were derived from these relationships using observations of CO, CO2, OA, and BC." –

***AUTHORS RESPONSE**: We agree with the reviewer. We will delete the whole sentence.*

L187: Temperature change even if very small should be included since it can impact gas-aerosol partitioning and evaporation of BB-POA. –

***AUTHORS RESPONSE:** Chamber temperature started at room temperature (around 20 °C or slightly above) and increased to a maximum of 30 °C after 5 hours of use when all the UV lights were turned on, with most of the increase happening within the first hour (Smith et al., 2019). The figure below is the temperature profile for different runs.*

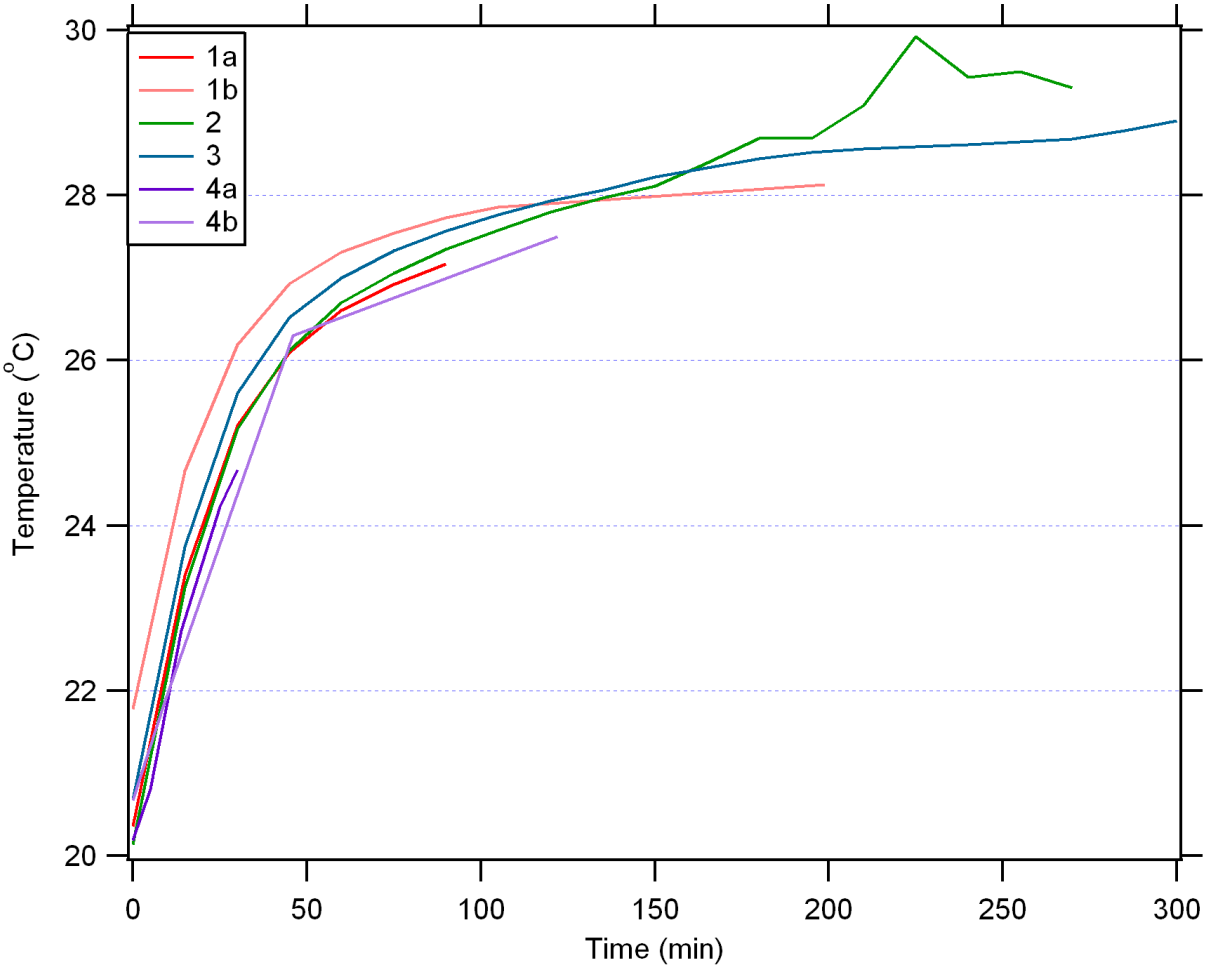

Fig. Temperature profile of the chamber. Runs 1b and 4b were done on the same day as runs 1a and 4a, respectively, with initial temperatures higher for 1b and 4b than 1a and 4a.

L216-217: Consider indicating what the aerosol number concentrations, and absorption and scattering coefficients typically were after 24-hr flushing and before start of a new expt. –

***AUTHORS RESPONSE**: Number concentrations were measured and must be below threshold values before a new experiment could begin. These values were typically around 25 – 40 particles cm^{-3} as measured by the CPC. Absorption and scattering at these low number concentrations were not measured and gives a typical background mass loading of 1 $\mu gm^{-3.}$*

L221: what does it mean that "The experiments were repeated after keeping the BB aerosol in the chamber overnight (24 hours) without the UV lights"? –

AUTHORS RESPONSE*: We are sorry for the typo. Now the sentence will read "For dark aging, measurements were repeated after 12 hours without the UV lights".*

L231: indicate manufacturer and level of purity –

AUTHORS RESPONSE*: These mixtures were composed of benzene (≥99.9%, Sigma-Aldrich), toluene (99.99%, Acros Organics), and ortho-xylene (99%, Alfa Aersar). This information will be added in the revised manuscript.*

L245-251: Typically, urban concentrations of VOCs are expressed as volumetric mixing ratios (ppmv or ppbv, etc). Is that not the case for the aromatics indicated here? If not, to clarify, you need to include ppmm or ppm by mass. If indeed the mixing ratios of 5:14:6 was ppmv based, then one expects different volumes (and different masses of them based on their density) of each to be injected and the calculation here is not correct. –

AUTHORS RESPONSE*: The reviewer is correct. There seems to have been some miscommunication among investigators during the experimental design of this particular experiment. See our response to the next comment, where both will be addressed.*

L254-256: what VOC mixing ratios were achieved in the bag so readers can compare them with the typical urban mixing ratios of these VOCs in Africa? –

AUTHORS RESPONSE*: The two paragraphs and the first table, from lines 239 – 263, will be replaced with the following text:*

"*To represent a polluted urban environment, we used emission inventory for urban environments from South Africa. This does not necessarily represent the east African emission inventory, but this serves as a baseline, since this is the only available data to us for the continent. This was obtained from South African Air Quality Information System (SAAQIS) and included concentrations of NOx, NO, NO_2, CO, O_3, benzene, toluene, ortho-xylene, and ethylbenzene for several South African Sites (Diepkloof, Kliprivier, Three Rivers, Sharpeville, Sebokeng, Zamdela, Thabazimbi, Lephalale, Phalaborwa, and Mokopane). The VOC data was obtained from the two weeks (M-F) of July 11 – 15 and July 18 – 22, which was in the middle of the peak burning season for South Africa for the year 2016. The urban areas (Diepkloof and Kliprivier) had combined average mixing ratios of 1.16, 3.48, and 1.44 ppbv for benzene, toluene, and o-xylene, respectively. Suburban areas (Three Rivers, Sebokeng, and Zamdela) had combined average mixing ratios of 1.69, 4.02, and 0.70 ppbv for the aforementioned gases, respectively. Interestingly, suburban regions had somewhat higher average benzene and toluene mixing ratios, though o-xylene was only half the average urban concentration.*

A mixture was prepared using equal by volumes of benzene, toluene, and o-xylene, and 2.5 mg was injected by syringe into a U-shaped glass tube attached to the chamber. This tube was then flushed by zero air into the chamber. This resulted in a mixing ratio of 29.7, 24.9, and 21.9

ppbv for benzene, toluene, and o-xylene, respectively. The concentration injected into the chamber was approximately 7 – 26 times more concentrated than values found from urban South African emissions and 6 – 18 times more concentrated than suburban values. The reason for these elevated levels was mostly due to sample preparation constraints, since the amounts needed for an exact match were too small for our scale to weigh appropriately. Concentrations in the chamber were intentionally higher than atmospheric conditions, in order to age the BB aerosol faster and accentuate the potential effect of SOA."

L267: what does "710 μm impactor inlet" mean? It seems 710 um is not related to the size cut. –

AUTHORS RESPONSE*: That is the diameter of the impactor used right before our DMA. We will rewrite the sentence as "BB aerosol was size selected for optical property measurements by passing the sample through an impactor inlet with a 710 μm nozzle (3.8 μm diameter cut point), charge neutralizer (TSI model 3081), and a long differential mobility analyzer (DMA) (TSI model 3080).*

L269- 270: how was the concentration of multiply charged particles accounted for? Those can significantly impact the measured optical coefficients given their larger physical size, even if their number concentration is not high. This is mentioned in lines 318-320, but still no consideration is given for correcting 200 nm particle concentrations.

AUTHORS RESPONSE*: As mentioned in the manuscript, concentration of multiply charged particles was not considered in this study. We completely agree with the reviewer that this will significantly impact the measured optical coefficients and cross sections. However, the impact of multiply charge particle on SSA is low (ratio of scattering to extinction coefficients/cross-section). We recently acquired an aerosol particle mass analyzer (APM) and after this comment was posted, we did an experiment using the APM in-line after the DMA and performed optical property calculation for freshly emitted BBA. Detail about the measurement strategy is given by Radney and Zangmeister, 2016). It was found that, due to the presence of multiply charged particles, our reported SSA values were overestimated by a maximum of 8% for 200 nm &300 nm particles. This information will be included in the revised manuscript.*

- Equation 2: need to define tau and tau0, sigma_ext and N(CRD). –

AUTHORS RESPONSE*: We thank reviewer for pointing this out. We will define those terms in Equation 2 in the revision.*

L294: Since the CPC is placed after the optical instrument, what is the fractionall loss of particles in the CRD and nephelometer? –

AUTHORS RESPONSE*: We thank reviewer for pointing this out. We used PSL sphere size standards to estimate the losses in CRDS and Nephelometer. The estimated particle losses in CRDS are 14.2, 14.7, and 11.4 percent for 200, 300, and 400 nm sizes, respectively, whereas for Nephelometer those losses are 8.6, 7.1, and 6.3 percent for those respective sizes. We accounted*

those losses in our final calculations of extinction and scattering coefficients, as discussed in depth in our previous publication (Singh et al., 2014) and this work is cited in the paper.

L316: it is worth indicating what each of these uncertainties are. –

***AUTHORS RESPONSE**: We will report those uncertainties. The sentence will now read "The calculation flow determining average extinction cross section (σ_{ext}), absorption cross section (σ_{abs}), and single scattering albedo (ω), was already described (Singh et al., 2014)(Singh et al., 2016). The estimated uncertainties are 11%, 15%, and 2.1% for σ_{ext}, σ_{abs}, and ω".*

L330-331: It's unclear what the CE value was and how it was determined for this one species. What assumptions need to be made to justify using the same CE for all the species? –

***AUTHORS RESPONSE**: We appreciate reviewer for mentioning this. This sentence will now read as "Since this work does not use mass loading in a quantitative way, we chose a collection efficiency of 1 for all species, similar to a previous study (Ng et al., 2011)".*

L340: this sentence needs to be rephrased "The optical properties were also measured as a function of different forms of aging: dark aged, photochemically and photochemically aged with added VOC's lights on in the presence of VOCs injected into the chamber before particles were introduced at both temperatures."

***AUTHORS RESPONSE**: We agree with reviewer. We will rephrase the sentence as "The optical properties of dark and photochemically aged aerosol were also measured".*

L351 and 363: section 2.3.1 is not in the paper.

***AUTHORS RESPONSE**: We thank reviewer for pointing out this typo. We will correct that as section 2.4 now.*

L357: How was concentration of BC taken into account to calculate the SSA? And how were the aerosols treated? Internal or external mixtures? These details need to be fully explained.

***AUTHORS RESPONSE**: We think there is a misunderstanding of what we did. We ran Mie model based on the RI of BC from Bond and Bergstrom, (2006) and RI of bulk aerosol from Levin et al, (2010). Based on these model result, we estimated the size selected SSA at 532 nm and did comparison with the SSA calculated from our measurements. The whole purpose of this was to point out two facts: 1. Aerosol formed during 800^{o} C burning are very absorbing (equivalent to pure BC) and 2. Due to the presence of multiply charge particles, our estimated SSA are biased, especially for lower size particles.*

L361-362: why would the impact of multiply charged particles not be present in lower combustion temperature samples? How different were the chamber size distributions under these conditions? The geometric mean for all fresh aerosols seems to be the same and 50 nm (Fig 1). - Figure 3. The legend needs to include the imaginary number indicator "i".

AUTHORS RESPONSE: *The typical particle size distribution (corrected for multiple charging) of two different burning temperatures is shown in Figure a. As depicted in the distributions, the higher temperature burn would be more impacted by multiply charged particles because the relative particle concentrations at 200 nm are lower compared to equivalent mobility particles with charges of +2 (314 nm) and +3 (418 nm). On the other hand, for lower temperature burn, concentration at 200 nm size is about 3.5 time larger than that of +2 (314 nm) and about 9 times larger than +3 (418 nm) size. All these facts suggest that there will be more impact due to multiply charged particles for the higher temperature burn than that of lower temperature burn as depicted in Figure a.*

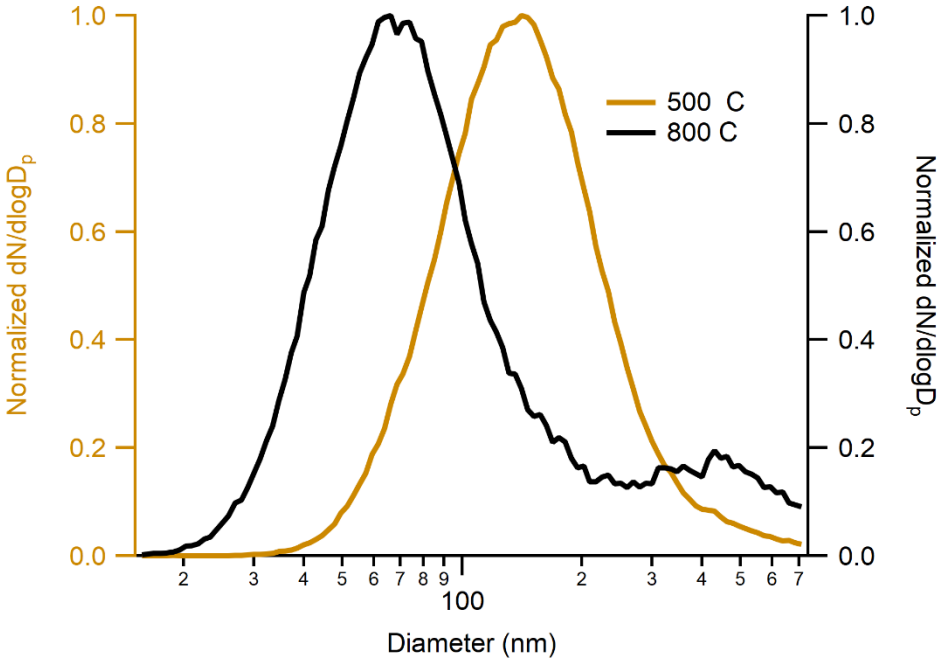

Figure a: Normalized particle size distribution for 500^o C and 800^o C burning cases.

We will replot Figure 1 with x-axis on log scale (shown below as Figure b), which shows the difference in the geometric mean diameter (GMD) of two different burning conditions. For the lower temperature case, it is typically about 85-90 nm whereas for higher temperature burn it is below 40 nm. We will update the legend for Figure 3.

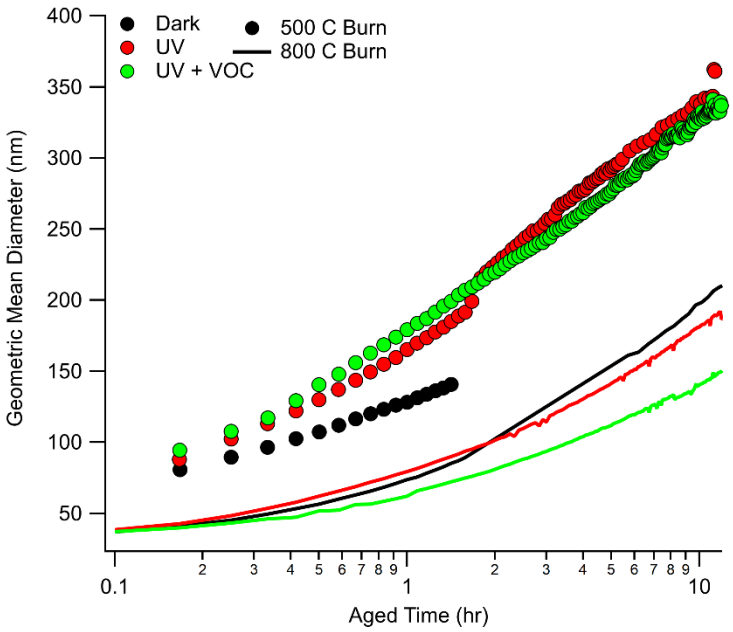

Figure b: Same as Figure 1 in the manuscript (x axis in log scale).

L380: Do the dashed lines show the uncertainties in SSA or the variability of the measurements, e.g., standard deviation of the average? Please be specific. –

***AUTHORS RESPONSE**: The dashed lines represent the propagated uncertainty (1 standard deviation) of the SSA, based on extinction and scattering coefficients. The scattering coefficient error is mainly produced by measurement variability from the nephelometer (~1%), while extinction errors from the CRDS are mainly influenced by variability in the ring-down time. This has been thoroughly described in our system characterization paper (Singh et al., 2014) cited in this paper.*

L391-392: Unlike what's mentioned here, SSA for eucalyptus aerosol is not uniformly higher or lower than other fuels; please correct this statement. This needs to be corrected in the conclusions as well. –
L382-400: The discussion on burn temperature and BC vs BrC emissions gets repeated; consider describing this dependence more concisely and to the point only once. -

***AUTHORS RESPONSE:** We agree with the reviewer. We will rewrite the two paragraphs (L382-409) and it will read as:*

"The range of SSA for different fuels combusted at 800^o C is 0.287 to 0.439, whereas the range for the same fuels combusted at 500^o C is 0.66 to 0.769. The average MCE for 800^o C burn cases is 0.974 ± 0.015 and that for 500^o C burn cases is 0.878 ± 0.008. These MCE values suggests that 800^o C burns are dominated by flaming phase and 500^o C burn cases are dominated by the smoldering phase of the burn. The flaming stage of the combustion produces more black carbon and smoldering stage produces more organic carbon (Christian et al., 2003; Ward et al., 1992), which explains the lower SSA values at higher temperature combustion. The impact of combustion temperature on aerosol can also be separated visually by looking at the color of the collected filter

samples, as shown in Figure S1. As evident from Figure S1, aerosol emitted from the 800^o C combustion looks black, whereas that from 500^o C combustion looks brownish, indicating a visual difference between black carbon dominated and organic carbon dominated emissions from same fuel under different combustion temperatures. Although the variation in SSA of the different fuels is dominated by the burning conditions, there occurs a clear but small dependence of SSA on fuel type under the similar burn conditions.

The range of SSA for combustion at 500^o C is comparable to previous studies with similar MCE values (Liu et al., 2014; Pokhrel et al., 2016). On comparing the SSA of the three different fuels under two different combustion temperatures, it is apparent that SSA is controlled more by the combustion conditions rather than the fuel types. There is a larger variation in SSA for the same fuel under two different combustion conditions, compared to the variation due to the inter fuel variability under the same combustion temperature. This result is consistent with a previous study, which showed that SSA is highly correlated with the EC/TC (proxy for the combustion conditions), even for a wide variety of fuels (Pokhrel et al., 2016). A complete list of sizes selected SSA of different fuels measured at two combustion temperatures and under different aging conditions is provided in Table S1."

Figure 5: why is the SSA for 400 nm included here whereas in other plots 300 nm observations were included? What is the reason for having much larger error bar on one of the data points? –

***AUTHORS RESPONSE**: The reason that* this data point seems to be an outlier in terms of its error is because, for that particular experiment, the standard deviation for the ring-down time of the blank was about double what it normally is, even compared to other wavelengths in the same experiment. This propagated to an SSA error of $\pm$0.113. The standard deviation of repeat SSA measurements was only ±0.008, as measurements during this experiment (Olive combusted at 500^o C) was extremely reproducible.

L414: The sentence related to the higher uncertainty needs to be rephrased. –

***AUTHORS RESPONSE**- We thank the reviewer again for pointing out this poorly constructed sentence. It will be rephrased as "This outlier could also be because of the higher error associated with the scattering measured by the nephelometer*."

L419-421: I don't think the example with actual values of SSA are needed. Also, the last sentence is stating something that has been known in the community for a long time; therefore, it's not worth reiterating or at least provide proper literature reference. –

***AUTHORS RESPONSE**: We agree with the reviewer. The sentence with the example is removed and the reference is provided in the last sentence and will read as "This suggests that by simply varying the combustion temperature, we can generate aerosols with very different optical properties and combustion efficiencies (Saleh et al., 2018;Liu et al., 2014)" in the revision*.

L431: Why is particle dynamic expected to be different at night compared to daytime such that it would influence nighttime oxidation differently? Please clarify.

AUTHORS RESPONSE*: The particle dynamics is different at night since there is, a pronounced increase of particle size and density which was also observed in previous laboratory and ambient measurements (Reid et al., 1998;Zhang et al., 2011). Even though the RH remains the same in our experiments, it was also shown that RH may facilitate heterogeneous reactions during the night (Li et al., 2015).*

L461: there's no basis for suggesting nitrogen-containing OA as opposed to other types of SOA were formed under these dark aging conditions since no information on composition was provided. Please rephrase/remove this in the Conclusions as well. –

AUTHORS RESPONSE*: We thank reviewer for pointing this. To make this clear, we are not suggesting nitrogen-containing OA as opposed to other types of SOA. On Line 460 we wrote that "We hypothesized secondary organic aerosol formation as a potential phenomenon happening during dark aging." Then at Line 461 we refer to the previous studies which concludes higher production of nitrogen containing OA and then we hypothesized this could be a possibility in our case. This was explained in more detail at the beginning of our response*.

L487: Section 2.2.1 includes description of photooxidation without additional VOCs –

AUTHORS RESPONSE: *We thank reviewer for pointing out the typo. This will be corrected to be 2.2.2*

L505-507: the explanation doesn't seem to be valid. Why can't it be that the SOA form these VOCs has the same optical characteristic as the SOA formed in the absence of the VOCs?

AUTHORS RESPONSE*: We agree that the wording here is strange. We will rephrase it in the revision as: "This is most likely because we took our measurements after 12 hours of aging, which was enough time for the scattering nature of the SOA produced during aging to drive measured SSA values to unity, regardless of the chemical pathway taken due to the addition of VOCs"*

L539: it appears that there was insignificant additional SOA formed from oxidation of aromatics that were added to the chamber. What was the NOx level in the experiments? Perhaps the high NOx conditions of the burns lead to low SOA yield from these precursors and therefore no significant SOA is observed. If results from aging in the presence of additional VOC were not conclusive, I suggest removing all the discussion related to it throughout the paper. –

AUTHORS RESPNSE: *NOx concentrations were only available during the chamber characterization experiments used for our previous paper. Equipment malfunctions prevented us from measuring this during chamber experiments. However, no additional NOx was added to the chamber during these experiments, only what was available due to combustion.*

L 516-517: I'm not following why continuous size-selection was not possible during these aging experiments

AUTHORS RESPONSE*: Unfortunately, our current setup does not allow continuous monitoring when particle sizes are being selected. Mainly, the volume of the nephelometer is too large compared with the relatively small flow rate provided by the WCPC. We have found that a flush time of at least 15 – 20 minutes is required to completely replace a sample within the nephelometer with a new one (when changing particle sizes, for example). At this rate, it takes about 4 hours to collect measurements for three different mobility diameters, including blank measurements, repeat measurements, and the time to flush between samples.*

References:

Bond, T. C. and Bergstrom, R. W.: Light Absorption by Carbonaceous Particles: An Investigative Review, Aerosol Sci. Technol., 40(1), 27–67, doi:10.1080/02786820500421521, 2006.

Levin, E. J. T., McMeeking, G. R., Carrico, C. M., Mack, L. E., Kreidenweis, S. M., Wold, C. E., Moosmüller, H., Arnott, W. P., Hao, W. M., Collett, J. L. and Malm, W. C.: Biomass burning smoke aerosol properties measured during Fire Laboratory at Missoula Experiments (FLAME), J. Geophys. Res. Atmos., 115(18), 1–15, doi:10.1029/2009JD013601, 2010.

Ng, N. L., Herndon, S. C., Trimborn, A., Canagaratna, M. R., Croteau, P. L., Onasch, T. B., Sueper, D., Worsnop, D. R., Zhang, Q., Sun, Y. L. and Jayne, J. T.: An Aerosol Chemical Speciation Monitor (ACSM) for routine monitoring of the composition and mass concentrations of ambient aerosol, Aerosol Sci. Technol., 45(7), 770–784, doi:10.1080/02786826.2011.560211, 2011.

Radney, J. G. and Zangmeister, C. D.: Practical limitations of aerosol separation by a tandem differential mobility analyzer-aerosol particle mass analyzer, Aerosol Sci. Technol., 50(2), 160–172, doi:10.1080/02786826.2015.1136733, 2016.

Singh, S., Fiddler, M. N., Smith, D. and Bililign, S.: Error analysis and uncertainty in the determination of aerosol optical properties using cavity ring-down spectroscopy, integrating nephelometry, and the extinction-minus-scattering method, Aerosol Sci. Technol., 48(12), 1345–1359, doi:10.1080/02786826.2014.984062, 2014.

Hartikainen, A., Yli-Pirilä, P., Tiitta, P., Leskinen, A., Kortelainen, M., Orasche, J., Schnelle-Kreis, J., Lehtinen, K. E. J., Zimmermann, R., Jokiniemi, J., and Sippula, O.: Volatile Organic Compounds from Logwood Combustion: Emissions and Transformation under Dark and Photochemical Aging Conditions in a Smog Chamber, Environmental Science & Technology, 52, 4979-4988, 10.1021/acs.est.7b06269, 2018.

Li, C., Ma, Z., Chen, J., Wang, X., Ye, X., Wang, L., Yang, X., Kan, H., Donaldson, D. J., and Mellouki, A.: Evolution of biomass burning smoke particles in the dark, Atmospheric Environment, 120, 244-252, https://doi.org/10.1016/j.atmosenv.2015.09.003, 2015.

Liu, S., Aiken, A. C., Arata, C., Dubey, M. K., Stockwell, C. E., Yokelson, R. J., Stone, E. A., Jayarathne, T., Robinson, A. L., DeMott, P. J., and Kreidenweis, S. M.: Aerosol single scattering albedo dependence on biomass combustion efficiency: Laboratory and field studies, Geophysical Research Letters, 41, 742-748, 10.1002/2013GL058392, 2014.

Reid, J. S., Hobbs, P. V., Ferek, R. J., Blake, D. R., Martins, J. V., Dunlap, M. R., and Liousse, C.: Physical, Chemical, and Optical Properties of Regional Hazes Dominated by Smoke in Brazil, J. Geophys. Res., 103, 32059, 1998.

Saleh, R., Cheng, Z., and Atwi, K.: The Brown–Black Continuum of Light-Absorbing Combustion Aerosols, Environmental Science & Technology Letters, 5, 508-513, 10.1021/acs.estlett.8b00305, 2018.

Singh, S., Fiddler, M. N., and Bililign, S.: Measurement of size-dependent single scattering albedo of fresh biomass burning aerosols using the extinction-minus-scattering technique with a combination of cavity ring-down spectroscopy and nephelometry, Atmospheric Chemistry and Physics, 16, 13491-13507, https://doi.org/10.5194/acp-16-13491-2016, 2016.

Smith, D. M., Fiddler, M. N., Sexton, K. G., and Bililign, S.: Construction and Characterization of an Indoor Smog Chamber for Measuring the Optical and Physicochemical Properties of Aging Biomass Burning Aerosols, Aerosol and Air Quality Research, 19, 467-483, 10.4209/aaqr.2018.06.0243, 2019.

Smith, D. M., Cui, T., Fiddler, M. N., Pokhrel, R., Surratt, J. D., and Bililign, S.: Laboratory studies of fresh and aged biomass burning aerosols emitted from east African biomass fuels - Part 2: Chemical properties and characterization, Atmos. Chem. Phys. Discuss., 2020, 1-30, 10.5194/acp-2019-1160, 2020.

Tiitta, P., Leskinen, A., Hao, L., Yli-Pirilä, P., Kortelainen, M., Grigonyte, J., Tissari, J., Lamberg, H., Hartikainen, A., Kuuspalo, K., Kortelainen, A. M., Virtanen, A., Lehtinen, K. E. J., Komppula, M., Pieber, S., Prévôt, A. S. H., Onasch, T. B., Worsnop, D. R., Czech, H., Zimmermann, R., Jokiniemi, J., and Sippula, O.: Transformation of logwood combustion emissions in a smog chamber: formation of secondary organic aerosol and changes in the primary organic aerosol upon daytime and nighttime aging, Atmos. Chem. Phys., 16, 13251-13269, 10.5194/acp-16-13251-2016, 2016.

Zhang, H., Hu, D., Chen, J., Ye, X., Wang, S. X., Hao, J. M., Wang, L., Zhang, R., and An, Z.: Particle Size Distribution and Polycyclic Aromatic Hydrocarbons Emissions from Agricultural Crop Residue Burning, Environmental Science & Technology, 45, 5477-5482, 10.1021/es1037904, 2011.

RESPONSES to REFEREE #2

Received and published: 17 March 2020

This manuscript presents measurements of single scattering albedo (SSA) of size-selected aerosols emitted from controlled combustion of African biomass fuels under three conditions: fresh emissions, dark aged aerosols and photo-chemically aged aerosols. Three types of wood fuels were combusted in a tube furnace at two different temperatures (500 C and 800 C) and an indoor smog chamber was used to age aerosols in clean and polluted (VOC rich) environments.

AUTHORS RESPONSE*: We thank the reviewer for the time he/she took to provide us with valuable suggestions. The authors feel that the reviewer either misunderstood our descriptions and overlooked some aspects of the paper. We will show this is indeed true in our detailed responses with relevant references to each question and comment. We feel that there is rush to dismiss and devalue the work and undermine the paper instead of giving us a chance to respond and clarify our claims. We hope our responses and explanations will convince the referee to make a different final determination.*

The authors claim that the significance of their work lies in providing optical and chemical characterization of a previous unstudied group of fuels that contribute significantly to aerosol emissions in Africa. However, there are no novel findings reported in this study and claims of significance are greatly overstated. While the particular fuels in this study might not have been characterized, there is a robust body of literature regarding the effect of combustion conditions on optical properties of emitted aerosols in controlled (example: Chen and Bond, 2010, ACP; Saleh et al., 2018, ES&T) as well as representative household use (Roden et al., 2006, ES&T; Chen et al., 2012, ES&T) settings. This study was limited by a lack of chemical characterization and SSA measurements limited to mid-visible wavelengths, and therefore could only reiterate the well-known effect of combustion temperature on absorption efficiency.

AUTHORS RESPONSE*.*

There is no doubt that emissions from African continent is a major source of atmospheric aerosol, but their optical properties are least studied compared to emissions from other regions. Even though there are several studies on the impact of burning conditions on optical properties, we don't have full understanding as to why certain fuels burn with higher efficiency. For example, savannah grass fires tend to be of flaming type while boreal fires tend to be of smoldering type (Saleh et al., 2014). In addition, optical properties (such as absorption per mass) also show fuel dependency (Chen and Bond, 2010). All these facts suggest that we need more studies on different unstudied group of fuels. A recent critical review by Hodshire et al. (2019) recommends the following: "(1) More smoldering fires within the laboratory setting should be studied. As well, methods to more closely match field burns should be developed, such as burning more compact fuels/larger amounts… (2) A wider sampling of fuels as laboratory studies have been focused predominantly on fuels that may exist in North American fires." This paper address both recommendations.

Regarding all the examples provided by the reviewer, work by Chen and Bond, 2010 was done at lower temperatures (max 360 ^{o}C) whereas Saleh et al. 2018 was done for propane not for

a biomass fuel. So, we think more studies are needed on biomass combustion. This work is presented as a two-part study, where this part focused on optical properties and chemical composition and characterization is presented in Part II, which is published in ACPD and we will refer the reviewer to the second part for a detailed discussion(Smith et al., 2020). Further integration of the two manuscripts will be done, and summaries from Part 2 will be incorporated into the revised manuscript.

Following the paragraph contrasting eucalyptus and acacia combusted at 800^o C, the following text will be added to line 393:

"In the companion paper to this (Part 2), methanol extracts from BBA collected on Teflon filters were analyzed by ultra-performance liquid chromatography interfaced to both a diode array detector and an electrospray ionization high-resolution quadrupole time-of-flight mass spectrometer (UPLC/DAD-ESI-HR-QTOFMS) in negative ion mode. This was used to determine the relative abundance and light-absorption properties of biomass burning organic aerosol constituents. MS analysis of BBA extracts from combustion at 800 °C revealed very little difference between the two fuel types, suggesting that there are either very few BrC species produced for either fuel under these combustion conditions, or there are numerous species that are essentially the same between the samples. However, given that Eucalyptus has a higher SSA than Acacia, this would suggest that Eucalyptus has more non-absorbing OA, or at least less absorbing than BC. Since it is Acacia that appears to have many more low-abundant organic constituents, several possibilities exist to explain these differences in SSA, as explored in more depth in Part 2. It is likely that Eucalyptus combustion products are not captured by some aspect of the extraction and UPLC/DAD-ESI-HR-QTOFMS analyses, that the observed differences in SSA are due to morphology differences, or some combination thereof. One potential explanation would be the presence of significant amounts of eucalyptol in the BBA, which is a large fraction of Eucalyptus oil, and is a cyclic ether that lacks any basic functionality amiable for negative ion mode analysis, has good solubility in alcohols, and does not absorb in the UV and visible. An examination of the UV-Visible spectra from the DAD shows no absorbing species in either region."

The following paragraph will be included in the manuscript following the discussion of fresh emissions produced by combusted at 500^o C, added to line 410:

"Chemical analysis revealed that, when combusted at 500 °C, eucalyptus and acacia had a variety of compounds in common, such as lignin pyrolysis products, distillation products, and cellulose breakdown products. Several lignin pyrolysis products and distillation products are more prevalent in Eucalyptus than Acacia, while pyrolysis products of cellulose and at least one nitroaromatic species were more prevalent in Acacia. Given that these lignin pyrolysis and distillation products are known chromophores and are more prevalent in Eucalyptus than Acacia, while Acacia has a higher abundance of non-chromophores derived from sugars and cellulose, one would assume that Eucalyptus would be more absorbing in the visible (i.e. have a lower SSA) than Acacia. Despite the chemical analysis not capturing absolute amounts of OA, Acacia was found to have an SSA that is higher than Eucalyptus by 0.1 to 0.2, which is consistent with chemical measurements. This suggests that Acacia has either larger absolute amounts of non-chromophore compounds or Eucalyptus has a greater quantity of chromophores whose absorptive properties extend to the 500 – 570 nm region of the visible spectrum. An analysis of the chromatographically-

integrated UV/Visible spectrum shows that there are chromophores whose absorption features peak ~290 nm and extend into the 500 – 570 nm region, though a normalized spectrum does not appear to show drastic differences between species."

Contrary to the reviewers comment we believe that our claim is not overstated for several reasons.

(1) Most current optical properties measurements are limited to a single or a few selected wavelengths. The accurate measurement of aerosol optical properties over the entire solar spectrum is a technological challenge. ***Our system allows measurement of optical properties at a wide range of wavelengths over most of the solar spectrum to determine "featured" absorption cross sections as a function of wavelength.*** *While most of the example provided by reviewer are limited to single wavelength our study was done for 500-570 nm range, and it is within our capability to conduct extinction measurements from 400-800 nm at any wavelength interval by simply changing mirrors. This represents a significant effort with the current dataset and lets its novelty be its justification. We haven't come across any experimental set up for aerosol optical properties measurement that can accomplish this.*

(2) We have more control of the combustion process. The tube furnace enables us to study different burning stages by controlling the temperature and speed of burning by adjusting the flow of air into the furnace. We have not come across aerosol optical measurement system that uses a tube furnace with so much control of the burning condition, as most studies simply burn an amount of fuel amenable for their measurement devices. The burn system closest to ours is the one reported by Chakrabarty's group (Sumlin et al., 2018b) where a heating coil is used to control temperature. The main difference is uniformity of the temperature throughout the furnace as opposed to a localized temperature in a coil and the control of the gas mixture flow during the burning. We have elected to present a range of combustion conditions to cover a range of combustion scenarios that could depend on different combustion circumstances (wildfires, land clearing, etc.).

(3) Soot generation was done using a tube furnace, which was attached to an indoor chamber, and samples were directly fed into the optical properties measurement system to measure the optical properties as a function of aging. While smog chambers are not new, such an integrated system is not common.

We are surprised that the reviewer overlooked all the experimental features which alone are significant. Moreover, we disagree with the reviewer that our study does not have novel findings.

1) *There has never been a laboratory study of BB aerosols from biomass fuels in the region that we are aware of.*
2) *We showed that by just changing burning temperature, the SSA of emitted aerosol differ very significantly for the same BB fuel. This was different than Saleh et al. 2018, which was done for propane not biomass fuel. We showed that nighttime aging (dark aging) increase the SSA of aerosol, which we think this is one of the very few studies to report that.*

In that sense, this work represents attempt towards filling the gaps in our understanding of biomass burning aerosol optical properties in this under-sampled and ignored part of the world. Africa is the single largest continental source of BB emissions, with recent studies estimating that it makes ~55% of the global contributions to BB aerosols (Ichoku et al., 2008;Roberts et al., 2009;Roberts and Wooster, 2008;Lamarque et al., 2010;van der Werf et al., 2010;Schultz et al., 2008). Measurement of optical properties of biomass fuels from the region is long overdue.

The aging experiments show that both dark and photochemical aging reduce the absorption efficiency of size-selected aerosols (photochemical more so than dark) but no chemical properties were measured to illuminate the mechanism of absorption loss.

AUTHORS RESPONSE*: In the accompanying paper, we analyzed methanol extracts from Teflon filters, as detailed in the excerpt above. Given that this is the main subject of Part 2, it wouldn't be appropriate to go into significant depth here, and we would refer the referee to the accompanying paper that is on ACPD for a detailed discussion. While measurements of dark aged samples were not performed, a summary of results from Part 2 regarding the light aged BBA will be provided and incorporated into the manuscript. With regards to photochemical aging, the text will be amended at line 504, as described* ***two comments down from this.***

Further, the aging results are only presented for 500 C aerosols because (Line 471): "Therefore, due to the very low number concentration and highly absorbing nature of the particles, the scattering coefficient at 800 C was below the detection limit of our nephelometer during the aging experiments." The authors propose that future studies will include these missing measurements (performed by increasing the amount of fuel burnt) but I am puzzled why these changes were not made for this study.

AUTHORS RESPONSE*: We tried the aging experiment with higher load and were not successful due to the limitation in the amount of fuel we can burn in our system at a single time. Furthermore, our current setup prohibits bulk aerosol measurement. This work is focused on conducting measurements for size selected particles. It is possible to perform these measurements for the entire size distribution, but this brings its own challenges and other parameters, such as changes in the size distribution itself, become unconstrained.*

There are similar problems with aging experiments in a polluted environment (Line 505: "This is because we took our measurements after 12 hours of aging, which seems long enough to characterize the impact of the added VOC due to aging in UV. This fact suggests that a more carefully controlled study is needed to accurately simulate the impact of urban pollution on aerosol single scattering albedo") that indicate that the authors did not rigorously handle their motivating hypotheses, leaving glaring holes in their manuscript.

AUTHORS RESPONSE: *This is hardly the case, though the authors admit that this could be phrased better. Starting at line 504 with the sentence "We attempted…", the remainder of this paragraph and the next (after Figure 7) will be replaced with the following text:*

"Despite the use of anthropogenic VOCs, a concentration larger than those average values found in urban and suburban regions of South Africa, no distinct effect was observed for SSA values of BBA produced during combustion at 500 °C. While it is possible that the relatively long aging time could obscure some of the effects due to the presence of VOCs, it is also possible that combustion products dominate molecular species and the effects of additional VOCs are insignificant. The later would suggest that anthropogenic pollution does not seem to affect the optical properties of BBA. Indeed, in examining the effects of aging on the chemical composition of BBA shows very few species that could be attributed to anthropogenic VOCs; specifically, only dihydroxyphthalic acid produced from xylene. For both Eucalyptus and Acacia, an isomer of dihydroxybenzene, such as resorcinol or catechol, was removed to the highest degree from the fresh BB aerosol upon photochemical aging. Generally, very few compounds were produced to a significant extent and both fuels were dominated by loss of chromatophoric lignin pyrolysis and distillation products. Not surprisingly, the associated absorbance from these chromophores, mostly from 200 – 350 nm, also attenuated with respect to age. This may be caused in part by the photo-bleaching effect created by irradiation of UV light for 12 hours, heterogeneous OH oxidation, and SOA formation of non-chromophores.

This fact suggests that a study with a higher temporal resolution is needed to simulate the impact of the VOCs on aerosol SSA, where continuous or much more frequent measurement are needed to determine impact of urban pollution on aerosol single scattering albedo. Such a study, using continuous measurements, is not possible for our setup when particles are also size selected. Like dark aged conditions, we were not able to estimate SSA for combustion at 800 ^{o}C due to the low particle concentration and highly absorbing nature of the aerosol. A chemical analysis of aged BBA produced at this temperature revealed very few changes, suggesting there are few molecular species produced by combustion at this temperature."

Indeed, this is substantiated later in the paper by the lack of OA enhancement from the presence of anthropogenic VOCs.

Aside from concerns about significance and study design, there are significant issues in how the manuscript is presented. Instances of grammatical errors and confusing sentence construction are far too many to enumerate but more importantly, several arguments/claims are not supported by findings in this study or citations from literature.

AUTHORS RESPONSE**:** *We thank reviewer for constructive comment and pointing out the grammatical errors. There is indeed no excuse for this and we will thoroughly review the manuscript to fix the grammatical issues and clarify confusing sentences.*

The authors establish that the fuels studied here are household fuels and acknowledge the potential differences between typical household use and controlled burning. They do not present any discussion of how findings from controlled combustion can be extended to a more realistic condition: this undermines the purported importance of their findings.

AUTHORS RESPONSE: *We thank reviewer for valuable comment. While laboratory studies provide opportunities for control over the environmental and chemical conditions, so we can examine the effect of changing single variable at a time, a limited number of fuel-specific comparisons can be made between the laboratory and field studies given the lack of adequate field*

studies in Africa. Recreating the atmospheric conditions of plumes in the field, is still a challenge though this is a long-term goal of our research group. We acknowledge that there are significant knowledge gaps that limit a full understanding of how field and laboratory observations can be reconciled. This should not be a reason not to do laboratory experiments, but rather the reason to do more of those so we can clearly understand the physics and chemistry that governs the observed variability. However, we added following discussion on L 98: "This study was done in more controlled environment and to extend the result from this kind of study to more realistic condition we apply our optical property result to previously proposed parameterization schemes."

Further, they designate their 800 C burn condition as flaming (a reasonable assumption) and 500 C burn as smoldering (which is much higher than smoldering temperatures in literature). These assumptions are not substantiated with any further evidence. The SSA values reported for smoldering appear too low for pure smoldering combustion (eg. - those in (Sumlin et al., 2018a) and I am not convinced that the authors ensured that they are not from mixed combustion conditions.

AUTHORS RESPONSE: *We agree with reviewer. There is no clear single line that separates the smoldering and flaming fires, and it is likely that there is a gradient of conditions as a function of temperature. The designation was made based on the observed colors of the filter samples and measured MCE's. The latter is, of course, quantitative and enables the comparison of this work to others. Changes will be made throughout the manuscript with 800 ^{o}C described as "flaming-dominated burning" and 500 ^{o}C as "smoldering-dominated burning". As evident from the estimated MCE, flaming dominated and smoldering dominated are valid descriptions.*

Line 415 (comparing SSA values here with previous studies) states: "This could explain why our SSA calculations for BrC was lower than expected". All measurements in this study are for total aerosols, BrC is mentioned without any justification.

AUTHOR RESPONSE: *We appreciated reviewer comments. We will replace BrC with the phase "smoldering-dominated aerosol" throughout the manuscript. We agree that aerosol emissions at 500 ^{o}C have contributions from black carbon and other organic/inorganic components*.

Many hypotheses are presented for the aging observations however the study was not conducted in a way that allows any plausible claims about "night-time formation or aromatic nitrogen containing compounds", for example. SOA formation is presented as a hypothesis for SSA reduction (Line 492) during photochemical aging but fragmentation of absorbing aerosols is not considered.

AUTHORS RESPONSE*: We thank reviewer for constructive comments. The reason for making hypothesis for SOA formation during dark aging was that the SSA increase in those experiments was driven by an increase in scattering cross section with no evidence of changes in absorption cross section, as mentioned in the manuscript (L 455-458). There is lots of evidence of nighttime chemistry resulting in relatively high amounts of nitrogen containing SOA (Hartikainen et al., 2018;Tiitta et al., 2016;Li et al., 2015). That is the reason we made a statement about this*

possibility for our experiments. We acknowledge that this is a rich subject area, and there could be a variety of chemical transformations, such as acid-catalyzed reactions.

Regarding reviewer comments on photochemical aging, we also talked about the possibility of fragmentation of absorbing aerosol. As stated on Line 494-95 "An increase in SSA is possible during photochemical aging due to degradation in brown carbon absorptivity (Sumlin et al., 2017). So, we think we were not sticking only to an SOA hypothesis. If the reviewer is referring to the physical fragmentation of aerosol, the authors are not familiar with this process, nor do we consider it very likely. If the reviewer is referring to "collapse" of aggregates into shapes that are more spherical, it's very unlikely that such large changes in SSA can be attributed to that process.

Finally, the choice of figure type for representing the results in figures 4, 6 and 7 is baffling to me: why are SSA values plotted over this very narrow range of wavelengths? Clearly, no wavelength dependence can be seen between 500 and 570 nm. I fail to see the purpose of multiple figures that contain a series of zigzagging flat lines.

AUTHORS RESPONSE: *Clearly, the purpose of those figures was to see the wavelength dependency, or lack thereof in this case. As previous studies (Sumlin et al., 2018a) showed that BrC has an impact on SSA with lower SSA at shorter wavelengths, though these measurements were performed at discrete wavelengths (like 405, 532, 600 etc.) and it was not quite clear that this range of wavelengths definitively shows a BrC effect on SSA. Most of the previous studies were limited to either 405, 532, 660, 780 nm measurements and the behaviors in between those wavelengths is typically assumed. Assuming something like a power-law dependence cannot realistically hold for a wide range of wavelengths. That's why we present whole range of SSA measurements between 500 to 570 nm which may appear as zigzag lines. Previous work in our laboratory shows that, even at this wavelength range, a wavelength-dependent SSA can be observed, and it should not be taken for granted or assumed that the range is too narrow for a wavelength-dependent conclusion to be made; only that the results are restricted to the most intense portion of the solar spectrum.*

References

Chen, Y. and Bond, T. C.: Light absorption by organic carbon from wood combustion, Atmos. Chem. Phys., 10, 1773–1787, 2010.

Saleh, R., Robinson, E. S., Tkacik, D. S., Ahern, A. T., Liu, S., Aiken, A. C., Sullivan, R. C., Presto, A. a, Dubey, M. K., Yokelson, R. J., Donahue, N. M. and Robinson, A. L.: Brownness of organics in aerosols from biomass burning linked to their black carbon content, Nat. Geosci., 7, 647–650, doi:10.1038/ngeo2220, 2014.

Hartikainen, A., Yli-Pirilä, P., Tiitta, P., Leskinen, A., Kortelainen, M., Orasche, J., Schnelle-Kreis, J., Lehtinen, K. E. J., Zimmermann, R., Jokiniemi, J., and Sippula, O.: Volatile Organic Compounds from Logwood Combustion: Emissions and Transformation under Dark and

Photochemical Aging Conditions in a Smog Chamber, Environmental Science & Technology, 52, 4979-4988, 10.1021/acs.est.7b06269, 2018.
Hodshire, A. L., Akherati, A., Alvarado, M. J., Brown-Steiner, B., Jathar, S. H., Jimenez, J. L., Kreidenweis, S. M., Lonsdale, C. R., Onasch, T. B., Ortega, A. M., and Pierce, J. R.: Aging Effects on Biomass Burning Aerosol Mass and Composition: A Critical Review of Field and Laboratory Studies, Environmental Science & Technology, 53, 10007-10022, 10.1021/acs.est.9b02588, 2019.

Ichoku, C., Giglio, L., Wooster, M. J., and Remer, L. A.: Global characterization of biomass-burning patterns using satellite measurements of fire radiative energy, Remote Sensing of Environment, 112, 2950-2962, https://doi.org/10.1016/j.rse.2008.02.009, 2008.

Lamarque, J. F., Bond, T. C., Eyring, V., Granier, C., Heil, A., Klimont, Z., Lee, D., Liousse, C., Mieville, A., Owen, B., Schultz, M. G., Shindell, D., Smith, S. J., Stehfest, E., Van Aardenne, J., Cooper, O. R., Kainuma, M., Mahowald, N., McConnell, J. R., Naik, V., Riahi, K., and van Vuuren, D. P.: Historical (1850–2000) gridded anthropogenic and biomass burning emissions of reactive gases and aerosols: methodology and application, Atmos. Chem. Phys., 10, 7017-7039, 10.5194/acp-10-7017-2010, 2010.

Li, C., Ma, Z., Chen, J., Wang, X., Ye, X., Wang, L., Yang, X., Kan, H., Donaldson, D. J., and Mellouki, A.: Evolution of biomass burning smoke particles in the dark, Atmospheric Environment, 120, 244-252, https://doi.org/10.1016/j.atmosenv.2015.09.003, 2015.

Roberts, G., Wooster, M. J., and Lagoudakis, E.: Annual and diurnal african biomass burning temporal dynamics, Biogeosciences, 6, 849-866, 10.5194/bg-6-849-2009, 2009.

Roberts, G. J., and Wooster, M. J.: Fire Detection and Fire Characterization Over Africa Using Meteosat SEVIRI, IEEE Transactions on Geoscience and Remote Sensing, 46, 1200-1218, 10.1109/TGRS.2008.915751, 2008.

Schultz, M. G., Heil, A., Hoelzemann, J. J., Spessa, A., Thonicke, K., Goldammer, J. G., Held, A. C., Pereira, J. M. C., and van het Bolscher, M.: Global wildland fire emissions from 1960 to 2000, Global Biogeochemical Cycles, 22, GB2002, 10.1029/2007GB003031, 2008.

Smith, D. M., Cui, T., Fiddler, M. N., Pokhrel, R., Surratt, J. D., and Bililign, S.: Laboratory studies of fresh and aged biomass burning aerosols emitted from east African biomass fuels - Part 2: Chemical properties and characterization, Atmos. Chem. Phys. Discuss., 2020, 1-30, 10.5194/acp-2019-1160, 2020.

Sumlin, B. J., Pandey, A., Walker, M. J., Pattison, R. S., Williams, B. J., and Chakrabarty, R. K.: Atmospheric Photooxidation Diminishes Light Absorption by Primary Brown Carbon Aerosol from Biomass Burning, Environmental Science & Technology Letters, 4, 540-545, 10.1021/acs.estlett.7b00393, 2017.

Sumlin, B. J., Heinson, Y. W., Shetty, N., Pandey, A., Pattison, R. S., Baker, S., Hao, W. M., and Chakrabarty, R. K.: UV–Vis–IR spectral complex refractive indices and optical properties of

brown carbon aerosol from biomass burning, Journal of Quantitative Spectroscopy and Radiative Transfer, 206, 392-398, https://doi.org/10.1016/j.jqsrt.2017.12.009, 2018a.
Sumlin, B. J., Oxford, C. R., Seo, B., Pattison, R. R., Williams, B. J., and Chakrabarty, R. K.: Density and Homogeneous Internal Composition of Primary Brown Carbon Aerosol, Environmental Science & Technology, 52, 3982-3989, 10.1021/acs.est.8b00093, 2018b.

Tiitta, P., Leskinen, A., Hao, L., Yli-Pirilä, P., Kortelainen, M., Grigonyte, J., Tissari, J., Lamberg, H., Hartikainen, A., Kuuspalo, K., Kortelainen, A. M., Virtanen, A., Lehtinen, K. E. J., Komppula, M., Pieber, S., Prévôt, A. S. H., Onasch, T. B., Worsnop, D. R., Czech, H., Zimmermann, R., Jokiniemi, J., and Sippula, O.: Transformation of logwood combustion emissions in a smog chamber: formation of secondary organic aerosol and changes in the primary organic aerosol upon daytime and nighttime aging, Atmos. Chem. Phys., 16, 13251-13269, 10.5194/acp-16-13251-2016, 2016.

van der Werf, G. R., Randerson, J. T., Giglio, L., Collatz, G. J., Mu, M., Kasibhatla, P. S., Morton, D. C., DeFries, R. S., Jin, Y., and van Leeuwen, T. T.: Global fire emissions and the contribution of deforestation, savanna, forest, agricultural, and peat fires (1997–2009), Atmos. Chem. Phys., 10, 11707-11735, 10.5194/acp-10-11707-2010, 2010.

Laboratory studies of fresh and aged biomass burning aerosols emitted from east African biomass fuels-PART 1-Optical properties

Damon M. Smith,[1,2,#] Marc N. Fiddler[3], Rudra P. Pokhrel[1], Solomon Bililign[1*]

1. Department of Physics, North Carolina Agricultural and Technical State University, Greensboro, NC, 27411 USA,
2. Applied Sciences and Technology Program, North Carolina A&T State University, Greensboro, NC 27411, USA,
3. Department of Chemistry, North Carolina Agricultural and Technical State University, Greensboro, NC, 27411, USA

Current address: Department of Chemistry and Physics, Western Carolina University, Cullowhee, NC 28723
* Correspondence: Bililignsol@gmail.com; Tel.: (+13362852328);

Abstract: An accurate measurement of the optical properties of aerosols is critical for quantifying the effect of aerosols on climate. Uncertainties persist and measurement results vary significantly. Biomass burning (BB) aerosols have been extensively studied through both field and laboratory environments for North American fuels to understand the changes in optical and chemical properties as a function of aging. There is a clear research need for a wider sampling of fuels from different regions of the world for laboratory studies. This work represents the first such study of the optical and chemical properties of three wood fuel samples used commonly for domestic use in east Africa. In general, combustion temperature or modified combustion efficiency (MCE) plays a major role on the optical properties of the emitted aerosols. For fuels combusted with MCE of 0.974 ± 0.015, referred to as flaming dominated combustion, the single scattering albedo (SSA) values were in the range between 0.287 to 0.439, while for fuels combusted with MCE of 0.878 ± 0.008 referred to as smoldering-dominated combustion the SSA values were in the range between 0.66 to 0.769. There is a clear but very small dependence of SSA on fuel type. A significant increase in the scattering and extinction cross-section (with no significant change in the absorption cross-section) was observed, indicating the occurrence of chemistry, even during dark aging for smoldering-dominated combustion. This fact cannot be explained by the heterogeneous oxidation in particle phase and we hypothesize that secondary organic aerosol formation is potentially happening during dark aging. After 12 h of photochemical aging, BB aerosol becomes highly scattering with SSA values above 0.9, which can be attributed to oxidation in the chamber. Aging studies of aerosol from flaming-dominated combustion were inconclusive due to the very low number concentration of aerosols. We also attempted to simulate polluted urban environments by injecting volatile organic compounds (VOCs) and BB aerosol into the chamber, but no distinct difference was observed when compared to photochemical aging in the absence of VOCs.

1 Introduction

The role of biomass burning (BB) aerosols on air quality, human health, cloud formation, and climate remain poorly quantified. BB aerosol play an important role in the earth's radiation budget and in the hydrological cycle by

Formatted: Font color: Auto
Deleted: temperature
Deleted: at 800° °C,
Deleted: single
Deleted: s
Deleted: XXX
Deleted: a
Deleted: in the range between
Deleted: and
Deleted: the SSA values
Deleted: at 500° °C, are
Deleted: s
Deleted: in
Deleted: XXX
Deleted: in the range between
Deleted: and
Deleted: , with eucalyptus producing aerosol with higher SSA than olive and acacia
Deleted: mostly dominated by scattering
Deleted: combustion at 500° C
Deleted:
Deleted: chemistry
Deleted: d
Deleted: as a
Comment [MNF1]: If aerosol is plural, there shouldn't be an 's'
Deleted: phenomenon
Deleted:
Deleted: Due to the very low number concentration of aerosols during a
Deleted: combustion at 800° C
Deleted:
Deleted: , the results
Deleted: ejecting
Deleted: , since measurements were done 12 hours
Deleted: after injection of VOCs

absorbing and scattering sunlight and by providing nuclei for cloud condensation (Crutzen and Andreae, 1991). There have been several estimates of the radiative forcing of BB aerosols ranging from 0.03 ± 0.12 W m^2 (Forster et al., 2007) to the most recent estimate of −0.2 W m^{-2} (Boucher, 2013). The uncertainty associated with the radiative forcing is in the range of –0.07 to –0.6 W m^{-2} (IPCC, 2014). This high level of uncertainty is associated with uncertainty in measuring the optical properties of BB aerosol (Andreae and Merlet, 2001;Koch et al., 2009;IPCC, 2014). In most cases, the measurements of aerosol optical properties are either limited to a specific source region or confined to a limited wavelength range. Internally versus externally mixed particles can have very different optical properties (e.g.,(Jacobson, 2000;Stier et al., 2006;Schwarz et al., 2008)). The processing of fire emissions leading to the eventual formation of secondary organic aerosols (SOA) is complex, including dilution, partial evaporation of the primary organic aerosols (POA) into gaseous species, photochemical reactions of organic species, partitioning of semi-volatile primary emissions into the condensed phase upon cooling, and multiphase chemical conversion (including cloud processing) (Bruns et al., 2016).

Furthermore, it is often wrongly assumed that the only two aerosols to contribute significantly to light absorption on a global scale are black carbon (BC) and mineral dust. Current climate models fail to recognize that organic aerosols (OA) is not purely scattering (Bond et al., 2011;Ma et al., 2012;Bahadur et al., 2012;Laskin et al., 2015). Rather, there is a growing amount of data indicating that a certain class of OA, known as brown carbon (BrC), can be commonly found on a global scale, particularly in urban environments, where it contributes significantly to the total aerosol absorption, specifically in the lower visible and ultraviolet wavelength range, where BC absorbs weakly (Chung et al., 2012;Kirchstetter et al., 2004;Yang et al., 2009;Laskin et al., 2015). Global simulations suggest that this strongly absorbing BrC contributes from +0.12 to +0.25 W m^{-2} or up to 19% of the absorption by anthropogenic aerosols (Feng et al., 2013;Brown et al., 2018;Saleh et al., 2015;Saleh et al., 2014).

The environmental and health costs of pollutants emitted from open biomass burning and cookstoves are significant and have been associated with human health effects, including early deaths and low infant birth weight. There is a strong evidence for acute respiratory illnesses such as asthma, and chronic obstructive pulmonary disease (COPD) associated with open biomass burning (Naeher et al., 2007;Stefanidou et al., 2008;Holstius et al., 2012;Johnston et al., 2012;Johnston et al., 2011;Elliott et al., 2013;Henderson et al., 2011;Delfino et al., 2009;Rappold et al., 2011;Sutherland et al., 2005;Smith and Pillarisetti, 2017). Wildfire can have health impacts well beyond the perimeter of the fire; even thousands of miles downwind (Spracklen et al., 2009).

This work is focused on biomass fuels from east Africa. It is estimated that nine out of ten, or 573 million people in sub-Saharan Africa, will remain without access to electricity by 2030 (Bank, 2019). The African continent is the largest source of BB emissions, with recent studies estimating African contributions to be ~55% of total global emissions of BB aerosols (Ichoku et al., 2008;Roberts et al., 2009;Roberts and Wooster, 2008;Lamarque et al., 2010;van der Werf et al., 2010;Schultz et al., 2008). African combustion emissions are expected to grow. For example, organic carbon (OC) emissions from Africa, are expected to make up 50% of the total global emissions in 2030 (Liousse et al., 2014). Africa currently has the fastest growing population in the world; projected to more than double between 2010 and 2050, and surpassing two billion (UN, 2011).

Deleted:
Deleted: ,
Deleted:
Deleted: of
Deleted:
Deleted: evolution
Deleted:
Deleted: ,
Deleted:
Deleted: As of 2019,
Deleted:

BB is a global phenomenon, and it was shown that the long-range transport of pollutants emitted from BB can affect air quality very far from the source (Edwards et al., 2006;Williams et al., 2012). Although the optical properties of BB aerosols emitted by biomass species native to North America have been extensively investigated (Hodzic et al., 2007;Yokelson et al., 2009;Liu et al., 2014;McMeeking et al., 2009;Levin et al., 2010;Mack, 2008;Mack et al., 2010), biomass fuels native to sub-Saharan Africa have only been studied during a few field campaigns (Eck et al., 2001;Liousse et al., 2010;Formenti et al., 2003). Due to the very limited available data, the models being used for air quality and climate change in Africa rely on global inventories, which are primarily collected from North America, Europe and Asia (Bond et al., 2004;Streets et al., 2004;Bond et al., 2007;Klimont et al., 2009;Lamarque et al., 2010;Klimont et al., 2013), and are not consistent with satellite observations over Africa (Liousse et al., 2010;Malavelle et al., 2011;Liousse et al., 2014).

To our knowledge, laboratory studies of the optical properties of BB aerosols from solid wood biomass fuels common for domestic use in east Africa have not been conducted. The only other African fuel studied were savannah grass from South Africa during FLAME-4 (Pokhrel et al., 2016) and savannah grass from Namibia and Brachystegia spiciformis from Zimbabwe during the Impact of Vegetation Fires on the Composition and Circulation of the Atmosphere (EFEU) project (Hungershoefer et al., 2008). With the exception of these two examples almost all reported laboratory studies have been focused predominantly on North American fuels (Hodshire et al., 2019). To improve air quality and climate change models for Africa, there is a need for laboratory studies to measure optical properties of BB aerosols from African fuel sources as the aerosols age and interact with polluted air that has the same chemical profile as African megacities and rural areas.

Smog chambers provide a controlled environment for a comprehensive study of aerosol optical properties, chemical and morphological evolution, and SOA formation. While fuel specific studies cannot be easily compared to wildfire field studies (Akagi et al., 2012), they can be used to compare emissions from domestic biomass use where the fuel type is known and is often not mixed. It is suggested that burn conditions influence emissions and aerosol mass (Yokelson et al., 2013;Liu et al., 2017) and may be a key difference between laboratory and field studies. This study was done in a more controlled environment. To extend the results from this kind of study to more realistic conditions, we compare our results to previously parameterization schemes. In our work, we use a tube furnace for initiating the burn, where we have full control of temperature, airflow, and material combusted. Comparative laboratory studies of BB aerosol optical properties using fuels from Africa and higher latitudes under varying conditions and background pollutant abundances and photochemical aging will provide information on factors most critical for radiative impacts of BB aerosols.

In the first part of his study, we report the results from three biomass fuels from east Africa considered for a systematic fuel-specific study of optical properties of BB aerosols under different aging and burning conditions using an indoor smog chamber. Optical properties were measured for BB aerosols produced under smoldering-dominated and flaming-dominated conditions for each fuel type. For each burn condition, we report the measured optical properties (i.e. scattering and extinction cross sections and single scattering albedo (SSA)) for fresh emissions, dark aged, photochemically aged, and photochemically aged with added VOC's to represent urban emissions from a representative African megacity.

Deleted: over Africa

Deleted: the author's

Deleted:

Deleted:

Deleted: apply

Formatted: Justified, Indent: First line: 0.5"

Deleted:

Deleted: and

Deleted:

Deleted: ,

Deleted:

2 Experimental methods

For this study, authentic fuel plants were obtained from east Africa and left under a hood to dry out for over a year, expecting to retain little to no moisture content. These samples were weighed on a calibrated analytical balance so that it would approximately yield a total aerosol loading representative of a scenario (urban, wildfire, etc.). During all the experiments, we normally burned 0.5 g of fuel, which produced about 600 to 800 μg m^{-3} of mass loading in the chamber. The mass loading was estimated by determining the total aerosol volume, based on measuring the volume distribution with a scanning mobility particle sizer (SMPS) and assuming a density of 1 g cm^{-3} for fresh aerosol.

2.1 BB aerosol generation

For laboratory samples, BB aerosols were generated by combusting wood samples in a tube furnace. This process has been described elsewhere in detail and is summarized here for clarity (Poudel et al., 2017;Smith et al., 2019). Samples with a mass of 0.5 g were typically used for experiments, which generally produces enough BB aerosol for optical property measurements without overloading any of the instruments. Samples as small as 0.1 g and as large as 5 g have been used before, with the maximum mass loading for the tube furnace near 10 g. Biomass samples were placed in a quartz combustion boat (AdValue Technology, FQ-BT-03), which was in turn placed at the center of the working tube inside the furnace (Carbolite Gero, HST120300-120SN). Oxygen content can be varied between ambient conditions and the oxygen-starved conditions found within forest fires by mixing air from a zero-air generator (Aadco Instruments, 747-30) with nitrogen. Flows from both gases are regulated by calibrated mass flow controllers (MFC, Sierra Instruments). For this work, only zero air was used at a flow rate of 10 sL min^{-1}. The average modified combustion efficiency (MCE) for the 500 °C burn was 0.878 ± 0.008, which is hereafter referred to as smoldering-dominated combustion. For 800 °C burn case the average MCE was 0.974 ± 0.015, which is hereafter referred to as flaming-dominated combustion. Unlike the heating coils used to initiate burning (Sumlin et al., 2018) where the temperature is uneven and localized, the tube furnace provides a uniform temperature throughout the sample.

The North Carolina Agricultural and Technical State University (NCAT) indoor smog chamber has a volume of 9.01 m^3 and is lined by Fluorinated ethylene propylene (FEP) Teflon. Two sides each have a bank of 32 ultraviolet (UV) lights (Sylvania, F30T8/350BL/ECO, 36"), for a total of 64 lamps. Emissions from combustion (gas and particles) were transferred to the smog chamber via heated (200° C), ¼ inch stainless steel tubing, after which they undergo cooling and dilution in a natural fashion rather than a stepwise process. A mixing fan was used to produces a well-mixed volume within 10 to 20 minutes after combustion. In these experiments, the fan ran for 10 minutes while smoke was being introduced to the chamber, then for another 10 minutes after the furnace had been disconnected from the chamber. The chamber was constantly diluted by zero air (from generator). The flow rate was varied depending on the sampling demands of instrumentation, but was usually around 4 L min^{-1} for a normal cavity ring down spectroscopy (CRDS) experiment.

2.1.1 Burning stages

Deleted: We utilized previously measured emission factors (EFs) (Akagi et al., 2011;Simoneit, 2002;Yokelson et al., 2013;Andreae and Merlet, 2001), such as 18.5±4.1 g PM_{10} kg^{-1} wood (dry weight) for tropical forest fuels (Akagi et al., 2011). For instance, to achieve a mass loading of 1100 μg m^{-3}, which is the mean loading found in urban/suburban residential locations (Oyem, 2010), 0.5 g of wood was burned in these experiments.

Deleted: all of

Formatted: Superscript

Formatted: Superscript

Deleted: These fuel samples were left under a hood to dry out for over a year and were expected to have little to no moisture content.

Formatted: Justified, Indent: First line: 0.5"

Deleted:

Deleted: A furnace temperature of 500 °C was used to represent the smoldering stage of a fire, hereafter referred to as smoldering dominated combustion, while 800 °C was used to represent the flaming stage, hereafter referred to as flaming dominated combustion. Although a continuum exists between these two stages, 800 °C was chosen for the flaming stage, since little to no smoldering occurs at this temperature, and the modified combustion efficiency (MCE) value was > 0.98. We could also visually clearly distinguish between brown and black carbon, produced at 500 ° C and 800 ° C, respectively, when collected on filter samples. (Sumlin et al., 2018),

Formatted: Font color: Auto

Deleted: propylene FEP

Deleted:

MCE were calculated from CO and CO_2 measurements. These measurements underwent external calibration with either a pure gas (for CO_2) or a certified standard (199.7 ppm for CO and 5028 ppm for CO_2, purchased from Airgas National Welders). Gas filter correlation analyzers from Thermo Scientific were used to measure CO and CO_2 (models 48C and 41C, respectively). The change in the CO and CO_2 concentration was determined by comparing average measurements before a burn took place, and after the burn, once measurements rose and stabilized. Averages of elevated concentration were taken soon after measurements stabilized, but before dilution could take place. Between 80s and 300s measurements at 10 Hz were averaged for the pre-burn state, and ~300s for the post-burn state. MCE was determined by the following equation:

$$MCE = \frac{\Delta[CO_2]}{\Delta[CO_2]+\Delta[CO]} \quad (1)$$

2.1.2 Indoor smog chamber and characteristics

The smog chamber was constructed to sample several particulate and gas-phase species. Ozone (O_3) was measured with a Thermo- Environmental Instruments UV photometer (model 49), and NO_x was measured with a Monitor Labs fluorescence analyzer (model 8840). The O_3 and NO_x analyzer signals were digitized with a DAQ (National Instruments, USB-6002) and the signal was displayed and stored via custom software (LabVIEW).

Several parameters concerning our chamber itself have already been determined and reported (Smith et al., 2019). Chamber performance is affected by the intensity and spectral character of radiation, surface-to-volume ratio, and nature and condition of the wall surface (Hennigan et al., 2011). For our chamber, wall-loss rates of NO, NO_2, O_3 and PM were determined. Total light intensity was determined in a separate experiment by measuring photolysis of NO_2 and knowing the spectral output of the UV lamps. The wall loss rates for NO, NO_2, and O_3 were found to be $(7.40 \pm 0.01) \times 10^{-4}$, $(3.47 \pm 0.01) \times 10^{-4}$, and $(5.90 \pm 0.08) \times 10^{-4}$ min^{-1}, respectively. The NO_2 photolysis rate constant was 0.165 ± 0.005 min^{-1}, which corresponds to a flux of $(7.72 \pm 0.25) \times 10^{17}$ photons nm cm^{-2} s^{-1} for 296.0 – 516.8 nm, and the particle deposition rate was $(9.46 \pm 0.18) \times 10^{-3}$ min^{-1} for 100 nm mobility diameter BB particles from pine (Smith et al., 2019). Total aerosol surface area peaks approximately 20 minutes after combustion, while total aerosol volume peaks approximately 45 minutes after combustion. The aerosol appears to be well mixed within 20 minutes of combustion, with the size distribution resolving into a single lognormal distribution. However, this distribution continues to shift towards larger particle sizes, even after remaining in the smog chamber for over 24 h. This shift could be due to loss of small particles due to diffusion, coagulation, etc. The gas and particle loss rates and other properties for our chamber are comparable to similar indoor smog chambers previously reported e.g. (Babar et al., 2016;Leskinen et al., 2015;Wang et al., 2014;Paulsen et al., 2005)). Chamber pressure and temperature did not vary much from room pressure and temperature during these experiments. Even when the chamber was clearly pressurized, our sensor was not sensitive enough to show a change in pressure. Chamber temperature started at room temperature (around 20 °C or slightly above) and increased to a maximum of 30 °C after 5 hours of use when all the UV lights were turned on, with most of the increase happening within the first hour (Smith et al., 2019).

Deleted: .

Deleted: A limitation of open burn experiments performed in large chambers is that the burning efficiency and fuel type are likely coupled (Liu et al., 2014;Pokhrel et al., 2016). To adjust for differences between laboratory and field measurements, relationships were determined for SSA and absorption angstrom exponent (AAE) against MCE or OA/(OA+BC), and SSA and AAE were derived from these relationships using observations of CO, CO_2, OA, and BC.

Deleted: ,

Deleted: ,

Deleted:

Deleted:

Formatted: Font:10 pt, Not Italic

Formatted: Font:10 pt, Not Italic

Growth of aerosol particle inside the chamber was represented as a growth in the geometric mean diameter (GMD) of the size distribution, as shown in Fig. 1. Aerosol growth in the chamber was expected to be due to coagulation, diffusional losses of particles, and condensation of the gases into existing particles. It is evident from the Fig. 1 that growth is larger for the photochemical aging conditions compared to the dark aging, indicating aerosol growth is due to condensation and subsequent chemical transformations. However, for flaming dominated combustion, growth in GMD is the same for dark and photochemical aging conditions, indicating that there was no condensational growth in those experiments.

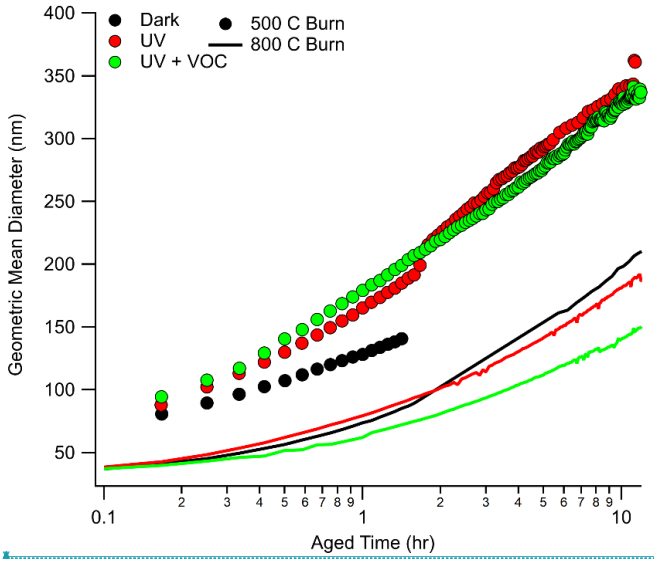

Figure 1: Growth of geometric mean diameter (GMD) as a function of photochemical age for eucalyptus under different burn and aged conditions represented in legend (black for dark aging, red for aging under light, and green for aging under light plus VOCs with solid line for flaming dominated combustion and filled circle for smoldering dominated combustion). Except for dark aging conditions, zero time represent the time at which light is turn on. For the lower temperature case, initial GMD was typically about 85-90 nm whereas for higher temperature burn it was below 40 nm.

2.1.3 Chamber cleaning

Between experiments, the smog chamber was flushed with zero air (from generator) for a minimum of 24 hours before starting the next experiment. The flow rate was varied somewhat, but was at least 10 L min^{-1} up to usually no more than 20 L min^{-1}. The furnace was also cleaned during this time and was reconnected to the chamber while it is still flushing. Even when precautions were taken, this can introduce additional contaminants, which were also

Deleted: -
Formatted: Indent: First line: 0"
Deleted: 800° C
Comment [RP3]: Grammar ?
Deleted:
Formatted: Font:10 pt, Font color: Text 1
Formatted: Font:Font color: Light Blue
Deleted: 800° C
Deleted: 500° C
Deleted: cases
Formatted: Font:9 pt, Not Italic
Deleted:
Formatted: Font:9 pt, Not Italic
Formatted: Font:9 pt, Not Italic
Formatted: Font:Font color: Text 1
Deleted:
Deleted: i

flushed out before a new burn. This additional flushing can take anywhere from 6 – 24 hours. When the chamber was not needed immediately, flushing continued at a constant 10 L min^{-1} to prevent room air from leaking into the chamber. Number concentrations were measured and were below 25 – 40 particles cm^{-3} as measured by the CPC before a new experiment began.

2.2 BB aerosol aging

2.2.1 Photochemical aging in a clean environment

For the purposes of these experiments, we define clean environment to be a smog chamber flushed out for 24 hours with clean air coming from the clean air generator. The only VOC's in the chamber come from the combustion of the fuel samples. Optical properties were measured using the procedure described below soon after the chamber was well mixed. For dark aging, the UV lights remained off, and measurements were repeated 12 hours after the introduction of BB aerosol in the chamber. For the photochemical aging, a new burn was made, and the particles were kept in the chamber for 12 hours with the UV lights on.

2.2.2 Photochemical aging in a polluted environment

A high degree of accuracy is required in setting up the conditions of an experiment and performing subsequent measurements. All gas-phase measurements were traceable to an analytical balance (calibrated yearly), NIST-certified flow meter (Mesa Laboratories, model Definer 220, calibrated yearly), NIST-certified stopwatch, and/or certified gas standard. Sample introduction accounted for the NO_x produced from BB itself. Individual hydrocarbons and hydrocarbon mixtures were prepared with the analytical balance. These mixtures were composed of benzene (≥99.9%, Sigma-Aldrich), toluene (99.99%, Acros Organics), and ortho-xylene (99%, Alfa Aersar), and were prepared at the time of use. The concentration in molecules/cm^3 was determined consistently by measuring the mass of syringes before and after injection into the chamber. Using measured chamber pressure and temperature, the concentration in pptv was estimated. All instruments were typically calibrated at the same time before a round of experimentation. NO and NO_2 were calibrated by passing certified standards through a calibrated MFC and mixing the standard with a calibrated flow of air in a ~30 mL glass mixing ball. Ozone was produced by passing air through an inline O_3 generator (UVP, model 97-0066-01). Using a calibrated NO_x instrument, the O_3 mixing ratio was determined by titrating it with NO to make NO_2. By measuring the O_3 signal, the calibration of O_3, in mV $ppmv^{-1}$, was performed.

To represent a polluted urban environment, we used an emission inventory for urban environments from South Africa. This does not necessarily represent the east African emission inventory, but this does serve as a baseline, since it is the only available data to us for the continent. This data was obtained from the South African Air Quality Information System (SAAQIS) and included concentrations of NO, NO_2, CO, O_3, benzene, toluene, ortho-xylene, and ethylbenzene for several South African sites (Diepkloof, Kliprivier, Three Rivers, Sharpeville, Sebokeng, Zamdela,

Deleted: need to be

Deleted: s

Deleted:

Deleted:

Deleted: The experiments were repeated after keeping the BB aerosol in the chamber overnight (24 hours) without the UV lights.

Deleted: are typically liquids, purchased at high purity

Deleted: . Mixtures

Deleted: were

Comment [MNF6]: Let's not be off by a factor of 1000

Deleted: m

Deleted: NOx,

Formatted: Subscript

Formatted: Subscript

Thabazimbi, Lephalalae, Phalaborwa, and Mokopnae). The VOC data was obtained from the two weeks (M-F) of July 11 – 15 and July 18 – 22, which was in the middle of the peak burning season for South Africa for the year 2016. The urban areas (Diepkloof and Kliprivier) had combined average mixing ratios of 1.16, 3.48, and 1.44 ppbv for benzene, toluene, and o-xylene, respectively. Suburban areas (Three Rivers, Sebokeng, and Zamdela) had combined average mixing ratios of 1.69, 4.02, and 0.70 ppbv for the aforementioned gases, respectively. Interestingly, suburban regions had somewhat higher average benzene and toluene mixing ratios, though o-xylene was only half the average urban concentration.

A mixture was prepared using equal by volumes of benzene, toluene, and o-xylene, and 2.5 mg of the mixture was injected by syringe into a U-shaped glass tube attached to the chamber. This resulted in a mixing ratio of 29.7, 24.9, and 21.9 ppbv for benzene, toluene, and o-xylene, respectively. The concentration injected into the chamber was approximately 7 – 26 times more concentrated than values found from urban South African emissions and 6 – 18 times more concentrated that suburban values. The reason for these elevated levels was mostly due to sample preparation constraints, since the amounts needed for an exact match were too small for our scale to weight appropriately. Concentrations in the chamber were intentionally higher than atmospheric conditions, in order to age the BB aerosol faster and accentuate the potential effect of SOA.

2.3 Optical properties measurement

BB aerosol was size selected for optical property measurements by passing the sample through an impactor inlet with a 710 µm nozzle (3.8 µm diameter cut point), charge neutralizer (TSI model 3081), and a long differential mobility analyzer (DMA) (TSI model 3080). Particles with mobility diameters centered at 200, 300, and 400 nm were selected by the DMA for this study. We verified that the standard deviations of the size distributions did not overlap (Poudel et al., 2017). The aerosol number density was measured by a water condensation particle counter (WCPC) (TSI model 3788), which was attached after the optical property instruments (shown in Fig. 2) and provided flow through the entire setup at 0.58 sL min^{-1}. Further, the DMA and WCPC could be rearranged and combined to form an SMPS, which was used to determine size distributions before taking optical property measurements.

Optical properties were measured using the extinction-minus-scattering technique (Weingartner et al., 2003;Bond et al., 1999;Sheridan et al., 2005), which uses CRDS to measure the total extinction of light and integrating sphere nephelometry to measure the scattering of light for the same aerosol sample (Moosmüller et al., 2005;Thompson et al., 2002;Thompson et al., 2008;Strawa et al., 2006). The details of the CRDS/Nephelometry optical properties measurement system is described in our recent work (Singh et al., 2014;Singh et al., 2016). A brief description is provided here. The extinction coefficient α_{ext} (m^{-1}) is > 1 and is defined as:

$$\alpha_{ext} = \frac{R_L}{c_{air}}\left(\frac{1}{\tau} - \frac{1}{\tau_0}\right) = \sigma_{ext} N_{CRD} \quad (2)$$

Deleted: ve

Deleted: To represent a polluted urban environment, we used emission inventory for urban environments from South Africa. This does not necessarily represent the east African emission inventory but this serves as a proxy since this is the only available data to us for the continent. This was obtained from South African Air Quality Information System (SAAQIS). NOx, NO, NO_2, CO, O_3, benzene, toluene, xylene, and ethylbenzene data for several South African Sites (Diepkloof, Kliprivier, Three Rivers, Sharpeville, Zamdela, Thabazimbi, Lephalale, Phalaborwa, and Mokopane) were obtained.

Urban Summary ... [1]

Deleted:

Deleted: air and particles from the smog chamber

Deleted: impactor inlet

Deleted: ’

Deleted:

Deleted: A

Deleted: a scanning mobility particle sizer (

Deleted:)

Deleted: a unitless number

Deleted:

where c_{air} is the speed of light in air, R_L is the ratio of mirror-to-mirror distance to the length of the cavity occupied by the sample, τ and τ_0 are the ring-down times, or the time it takes to reach $1/e$ of the original light intensity, of the sample and the blank measurement, respectively, σ_{ext} is the extinction cross-section of the aerosol in m^2, and N_{CRD} is the number concentration of the aerosol.

After being size selected, aerosol enter the ring-down cavity, where extinction was measured by passing a laser beam coupled to the cavity mode through the sample volume. The 355 nm beam from a Continuum Surelite I-20 Nd:YAG laser (at 20 Hz) pumps an optical parametric oscillator (OPO) laser, which can produce a range of wavelengths. For this study, we used a wavelength range of 500 to 570 nm and a single set of mirrors. Highly reflective mirrors confine most of the laser intensity within the CRDS, with a photomultiplier tube measuring the intensity of the light exiting the mirror after each round trip inside the cavity. Extinction is determined from the decay of light intensity exiting the mirrors. Our system allows measurement of optical properties at a wide range of wavelengths over most of the solar spectrum to determine "featured" extinction cross sections as a function of wavelength.

A purge flow of nitrogen was used to keep the mirrors clean. After the CRDS, the aerosols enter a integrating nephelometer (TSI, model 3563), where scattering is measured at three wavelengths (centered at 453, 554, and 698 nm. Lastly, the number density of the particles was measured by the WCPC, as stated above. As previously reported by Singh et al. (2014), estimated particle losses in the CRDS are 14.2, 14.7, and 11.4% for 200, 300, and 400 nm particle sizes, respectively, and estimated losses in the nephelometer are 8.6, 7.1, and 6.3% for the aforementioned sizes, respectively.

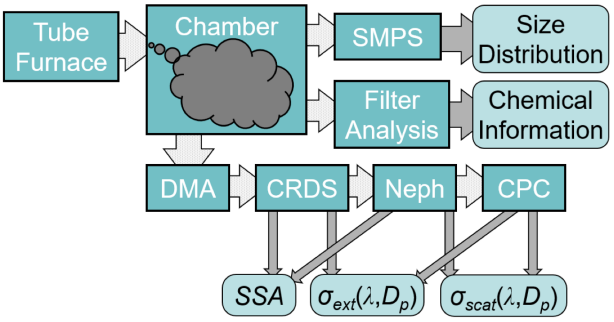

Figure 2. Scheme and flowchart for optical properties measurement

All flows, except the DMA sheath flow, are calibrated against a NIST-certified flow meter (Mesa Laboratories, model Definer 220) that is factory calibrated on a yearly basis and has a listed accuracy of < 1 %. Figure 2 describes the flowchart of the experiments.

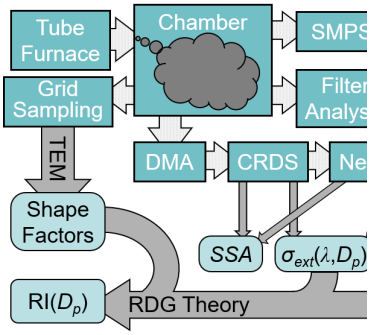

2.4 Error analysis of optical properties measurements

In our previous work (Singh et al., 2014) we have comprehensively and holistically accounted for known sources of random and systematic errors and developed a statistical framework for including the contributions to random error. The combined extinction cross section uncertainty (10 – 11%) was largely dominated by CPC

Deleted: and
Deleted: *d*
Formatted: Font:Italic
Formatted: Font:Italic
Formatted: Font:Italic, Subscript
Formatted: Font:Italic
Deleted: repectively
Formatted: Font:Italic
Formatted: Font:Italic, Subscript
Deleted: coefficient
Formatted: Font:Italic
Formatted: Font:Italic, Subscript
Deleted: resulting in a unitless value >1
Deleted: 8
Formatted: Font:10 pt, Not Bold, Not Italic
Deleted: absorption
Formatted: Font:10 pt, Not Bold, Not Italic
Deleted: se
Deleted: the
Deleted:) by three different photomultiplier tubes, each of which having a different dichroic filter.
Deleted:
Deleted:
Deleted: .
Deleted:

measurement error (10%). The calculation flow for determining the average extinction cross section (σ_{ext}), absorption cross section (σ_{abs}), and single scattering albedo (ω), was already described (Singh et al., 2014). The estimated uncertainties are 11%, 15%, and 2.1% for σ_{ext}, σ_{abs}, and ω, respectively.

The DMA can often allow multiply charged particles to pass through, that can result in artificially large measured cross sections, even for small number densities (Uin et al., 2011). Other groups have shown that measured extinction coefficients exceeded the predicted ones for 100 and 200 nm particles, which are most affected by the "multiple size–multiple charge" problem (Radney et al., 2009). As such, only particles 200 nm or greater were considered in this work. However, even with 200 nm particles, it has been shown that a small DMA sizing error can still produce significant changes in the extinction (Radney et al., 2013). In principle, errors in the DMA must be corrected (Miles et al., 2011;Toole et al., 2013). However, we did not make corrections due to DMA sizing error in this work.

2.5 Aerosol chemical speciation monitor (ACSM)

An aerosol chemical speciation monitor (ACSM; Aerodyne Research Inc., USA) was used to measure the chemical composition of sub-micron non-refractive particulate mass. Details about the ACSM can be found elsewhere (Ng et al., 2011). Briefly, dry aerosol from the chamber was sampled into the ACSM through a critical aperture with a diameter of 100 µm at a flow rate of 85 mL min^{-1}. The recorded data was processed using the ACSM local toolkit (v.1.6.0.3) for Igor Pro. Since this work does not use mass loading in a quantitative way, we chose a collection efficiency of 1 for all species, similar to a previous study (Ng et al., 2011).

3 Results and discussion

3.1 Optical properties measurements.

Aerosol optical properties, namely scattering and extinction coefficient for size selected aerosol, were measured for three different east African fuels. The selected fuels (eucalyptus, olive, and acacia) represent the most common trees in east Africa used for domestic use, which contributes to significant aerosol loading. Each fuel was burned at two different combustion temperatures (500 °C and 800 °C) to investigate the impact of ignition temperature on aerosol optical properties and chemical composition. The optical properties of dark and photochemically aged aerosol were also measured. In this paper, only the results from smoldering-dominated combustion under all aging conditions and the results of the fresh flaming-dominated combustion samples are reported. SSA values were measured for size selected particles having mobility diameters of 200, 300 and 400 nm.

3.2 Impact of size on SSA

SSA was calculated by taking the ratio of scattering coefficient to the extinction coefficient measured for the wavelength range from 500 − 570 nm at 2.0 nm interval. Calibration of the system and the error analysis in the

Deleted: and their errors

Deleted:

Deleted: show an apparent increase

Deleted: measurements from will be more impact by multiply charged particles those from the . ... [2]

Deleted: from one of the species to serve as a representative for all the species

Deleted: °

Deleted: °

Deleted: . The optical properties of dark and photochemically aged aerosol were also measured as a function of different forms of aging: dark aged, photochemically and photochemically aged with added VOC's lights on in the presence of VOCs injected into the chamber before particles were introduced at both temperatures. In this paper, only the results from the combustion at 500° Csmoldering dominated combustion under all aging conditions and the results of the fresh flaming dominated combustion samples combusted at 800° C are reported. SSA values were measured for someize selected particles having mobility diameters of 200, 300, and 400 nm

Deleted: particles

Deleted: cross-section

Deleted: cross-section

calculation of SSA from the experimental measurements is described in section 2.4. We calculated the scattering coefficients at the CRDS wavelength range by using the scattering angstrom exponent from the measured scattering coefficients.

Sub-micron aerosol shows size-dependent SSA values in visible wavelengths. Size-selected SSA values estimated in this study are compared with the size selected SSA valued predicted by Mie theory at 532 nm wavelength for both combustion temperature, as shown in Figure 4. Refractive indices (real and imaginary parts) were chosen to represent black and brown carbon samples based on values found by Bond and Bergstrom, (2006) and Levin et al. (2010). Figure 3 also shows the SSA of size-selected aerosol from different fuels combusted under different temperatures and the SSA of size-selected aerosol predicted from Mie theory. While no pronounced size dependence was observed for flaming dominated aerosols, contrary to what was predicted by Mie theory, the SSA does show size dependence for smoldering dominated aerosols. This may be due to the impact of multiply charged aerosol not discriminated by the DMA. We did not make corrections due to multiply charged particles in this work, as described in section 2.4. However, the impact of multiply charged particles on SSA is generally small for larger particles considered in this work, which have diameters of 300 or 400 nm. We have verified that the impact of multiply charged particle on SSA is low. This was done using an Aerosol Particle Mass analyzer APM (Kanomax APM 3602) in-line after the DMA with subsequent optical property measurements for freshly emitted BBA. Detail about the measurement strategy is given by Radney and Zangmeister, 2016). It was found that, due to the presence of multiply charged particles, our reported SSA values were overestimated by a maximum of 8% for 200 nm and 300 nm particles.

The impact due to multiply charged particles is more significant for the higher temperature (flaming-dominated) burn than that of lower temperature (smoldering-dominated burn). The typical particle size distribution (corrected for multiple charging) of two different burning temperatures is shown in Figure S1.

Deleted: 3.1

Formatted: Font:Not Bold

Deleted:

Formatted: Font:Not Bold

Deleted:

Formatted: Heading 2, Pattern: Clear (White)

Formatted: Font:Not Bold

Comment [MNF11]: Calculated? I would call these numbers better than estimates.

Formatted: Font:Not Bold

Formatted: Font:Not Bold

Deleted: 3

Formatted: Font:Not Bold

Deleted:

Deleted:

Deleted:

Deleted: 3

Formatted: Font:Not Bold

Deleted: samples combusted at 800°C

Deleted: ,

Deleted: samples combusted at 500°C

Formatted: Font:Not Bold

Deleted: 3.1

Formatted: Font:Not Bold

Deleted: We verified this in an experiment

Deleted: and performed

Deleted: calculation

Comment [MNF12]: There's a parenthesis missing here

Deleted: &

Deleted: A recently acquired aerosol particle mass analyzer (APM) was placed in-line after the DMA to perform optical property calculations for freshly emitted BB aerosol, using the measurement strategy given by Radney and Zangmeister (2016). It was found that, due to the presence of multiply charged particles, our reported SSA values were overestimated by a maximum of 8% for 200 nm and 300 nm particles.

Deleted:

Deleted: These comparisons are depicted in Fig. 3.

Formatted: Font:Not Bold

Formatted: Font:Helvetica, 18 pt, Font color: R,G,B (32,33,36), Pattern: Clear

Formatted: Heading 2, Pattern: Clear (White)

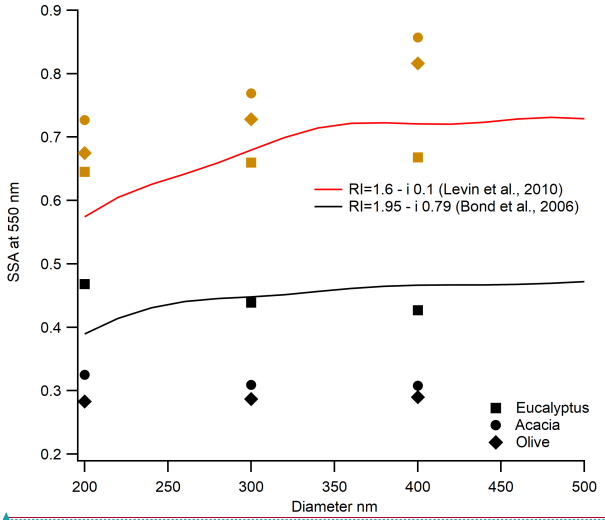

Figure 3: Impact of aerosol particle size on SSA. The solid red line is modeled SSA using Mie theory and the refractive index from Levin et al. (2010), representing typical BB emission, and black line is modeled SSA by Mie theory using refractive index from Bond et al. (2006), representing black carbon. Neither line is a fit to the data. Symbols are the different fuel types represented in the legend with black color for flaming dominated combustion and brown color for smoldering dominated combustion.

.

3.3 Single scattering albedo of freshly emitted aerosol

Figure 4 shows plot of SSA vs wavelength of light for freshly emitted 300 nm size aerosol from the different fuels at two different combustion temperatures (MCEs). The 200 and 400 nm particles show a similar behavior. The results show no wavelength dependence of SSA in the measured wavelength range of 500-570 nm at both combustion temperatures. The dashed lines represent the propagated uncertainty (1 standard deviation) of the SSA, based on extinction and scattering coefficients. The extinction errors from the CRDS are mainly influenced by variability in the ring-down time. The SSA shows dependence on fuel type even under the same combustion condition. This was consistent for all particle sizes investigated.

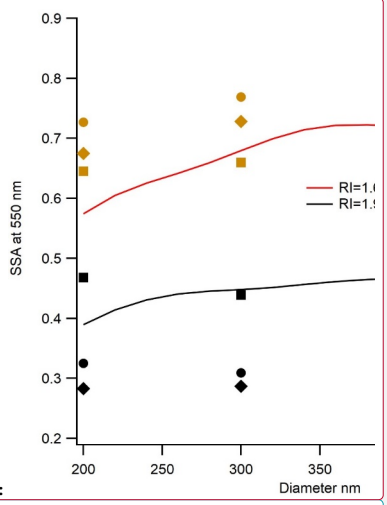

Deleted:

Formatted: Font:10 pt, Font color: Text 1, Pattern: Clear (White)

Comment [MNF14]: There's a weird blue line going across the lower figure

Deleted: **3**:

Deleted: using

Deleted: 800° C burn

Deleted: 500° C burn

Deleted: 4

Deleted: the SSA

Deleted: of freshly

Deleted: The

Deleted:

Deleted:

Deleted: . However, SSA

Formatted: Pattern: Clear

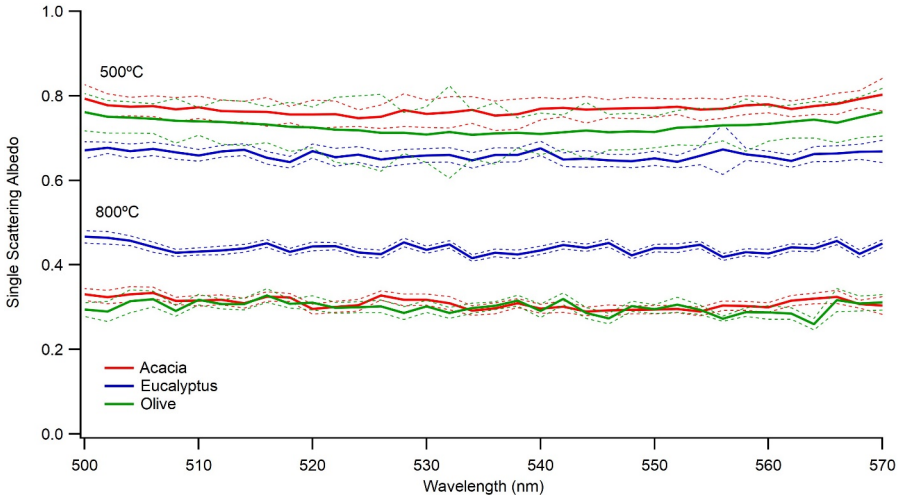

Figure 5: Single scattering albedo of 300 nm size-selected aerosol emitted at combustion temperatures of 500 °C and 800 °C. Solid blue, green, and red lines are for the average SSA from the three measurements and the dotted lines are the corresponding uncertainties (1 standard deviation) in the measured SSA.

The range of SSA values for flaming dominated combustion of different fuels is 0.287 to 0.439, whereas the range for the same fuels during smoldering dominated combustion is 0.66 to 0.769. The average MCE for flaming dominated combustion is 0.974 ± 0.015, while the average for smoldering dominated combustion is 0.878 ± 0.008. These MCE values suggest that combustion at 800 °C is dominated by the flaming stage of combustion, which produces more BC, and combustion at 500 °C is dominated by the smoldering stage of combustion, which produces more OC (Christian et al., 2003;Ward et al., 1992). This explains the lower SSA values at higher combustion temperatures. The impact of combustion temperature on aerosol properties can also be separated visually by looking at the color of the collected filter samples, as shown in Figure S2. As evident from Figure S2, flaming dominated aerosol looks black, whereas smoldering dominated aerosol looks brownish, indicating a visual difference between BC dominated and OC dominated emissions from the same fuel under different combustion temperatures.

The range of SSA for smoldering dominated combustion is comparable to previous studies with similar MCE values (Liu et al., 2014;Pokhrel et al., 2016). On comparing the SSA of the three different fuels under two different combustion temperatures, it is apparent that SSA is controlled more by combustion condition rather than fuel type. Although there appears a small but clear dependence of SSA on fuel type, there is a larger variation in SSA for the same fuel under two different combustion conditions, compared to the variation due to the inter fuel variability under the same combustion temperature. This result is consistent with a previous study, which showed that SSA is highly correlated with the ratio of elemental carbon to total carbon (a proxy for the combustion condition), even for a wide

Deleted: 4:
Deleted: o
Deleted: o
Formatted: Not Superscript/ Subscript
Formatted: Not Superscript/ Subscript
Comment [RP17]: In response we wrote it is propagated uncertainty based on ext and scat coefficient. It doesn't read like that here.
Deleted: 1
Deleted: 1
Deleted: the
Deleted: s
Deleted: the
Deleted: s
Deleted: s
Deleted: s

variety of fuels (Pokhrel et al., 2016). A complete list of size-selected SSA of different fuels measured at two combustion temperatures and under different aging conditions is provided in Table S1.

In the companion paper to this (Smith et al., 2020) methanol extracts from BB aerosol collected on Teflon filters were analyzed by ultra-performance liquid chromatography interfaced to both a diode array detector and an electrospray ionization high-resolution quadrupole time-of-flight mass spectrometer (UPLC/DAD-ESI-HR-QTOFMS) in negative ion mode. This was used to determine the relative abundance and light absorption properties of BB organic aerosol constituents. MS analysis of BB aerosol extracts from flaming dominated combustion revealed very little difference between the two fuel types, suggesting that there are either very few smoldering dominated aerosol species produced for either fuel under these combustion conditions, or there are numerous species that are essentially the same between the samples. However, given that Eucalyptus has a higher SSA than Acacia, this would suggest that Eucalyptus has more non-absorbing OA, or at least less absorbing than BC. Since it is Acacia that appears to have many more low-abundant organic constituents, several possibilities exist to explain these differences in SSA, as explored in more depth in the companion paper (Smith et al., 2020). It is likely that Eucalyptus combustion products are not captured by some aspect of the extraction and UPLC/DAD-ESI-HR-QTOFMS analyses, that the observed differences in SSA are due to morphology differences, or some combination thereof. One potential explanation would be the presence of significant amounts of eucalyptol in the BB aerosol, which is a large fraction of Eucalyptus oil, and is a cyclic ester that lacks any basic functionality amiable for negative ion mode analysis, has good solubility in alcohols, and does not absorb in the UV and visible spectrum. An examination of the UV-visible spectra from the DAD shows no absorbing species in either region.

Chemical analysis revealed that for smoldering dominated combustion, Eucalyptus and Acacia had a variety of compounds in common, such as lignin pyrolysis products, distillation products, and cellulose breakdown products. Several lignin pyrolysis products and distillation products are more prevalent in Eucalyptus than in Acacia, while pyrolysis products of cellulose and at least one nitroaromatic species were more prevalent in Acacia. Given that these lignin pyrolysis and distillation products are known chromophores and are more prevalent in Eucalyptus than in Acacia, while Acacia has a higher abundance of non-chromophores derived from sugars and cellulose, one would assume that Eucalyptus would be more absorbing (i.e. have a lower SSA) than Acacia in the visible spectrum. Despite the chemical analysis not capturing absolute amounts of OA, Acacia was found to have an SSA that is higher than Eucalyptus by 0.1 to 0.2, which is consistent with chemical measurements. This suggests that Acacia has either larger absolute amounts of non-chromophore compounds or Eucalyptus has a greater quantity of chromophores whose absorptive properties extend to the 500 – 570 nm region of the visible spectrum. An analysis of the chromatographically-integrated UV/Visible spectrum shows that there are chromophores whose absorption features peak near ~290 nm and extend into the 500 – 570 nm region, though a normalized spectrum does not appear to show drastic differences between species.

Figure 5 shows the SSA plotted as a function of MCE at 532 nm. Overall, our values of SSA agree well with the previous studies (Pokhrel et al., 2016;Liu et al., 2014) with some outliers. This could potentially be because we are comparing results for size-selected, as opposed to bulk, aerosols. In general, the variation of the SSA with MCE

Deleted: complete list of size

Deleted: s

Deleted: The measured SSA values for 800° C combustions were below 0.5, which indicates highly absorbing aerosol and corresponds to aerosol dominated by black carbon (Pokhrel et al., 2016). The calculated MCE (average from 12 different burns 0.974 ± 0.015) also supports the fact that aerosol emitted from combustion at 800° C represents the flaming stage, which is dominated by BC. The flaming stage of combustion produces more black carbon and less organic carbon which explains the lower values of SSA at visible wavelengths. The impact of combustion temperature on aerosol can be separated visually by looking at the color of the collected filter samples as shown in Fig. S1. As evident from Fig. S1, aerosol emitted from the 800° C combustion looks black whereas that from 500° C combustion looks brownish, indicating a visual difference between black and brown carbon emitted from same fuel under different combustion temperatures. Under the same combustion conditions and airflow, there is a clear but small dependence of SSA on fuel type with eucalyptus producing aerosol with higher SSA than olive and acacia. ... [3]

Deleted: (Part 2),

Deleted: Part 2.

Formatted: Indent: First line: 0.5"

Formatted: Indent: First line: 0"

Deleted: 5

Deleted: estimated

Deleted: vs

from the size-selected and bulk aerosol show a consistent behavior, with higher SSA for the lower MCE cases and lower SSA for higher MCE cases. As mentioned earlier, there occur some variabilities in SSA and MCE values even for the same combustion temperature. This could be due the dependence of SSA and MCE on fuel type or due to factors that we are not aware of. In general, however, combustion temperature plays a major role in the optical property of the emitted aerosol. This suggests that by simply varying the combustion temperature, we can generate aerosols with very different optical properties and combustion efficiencies (Saleh et al., 2018;Liu et al., 2014).

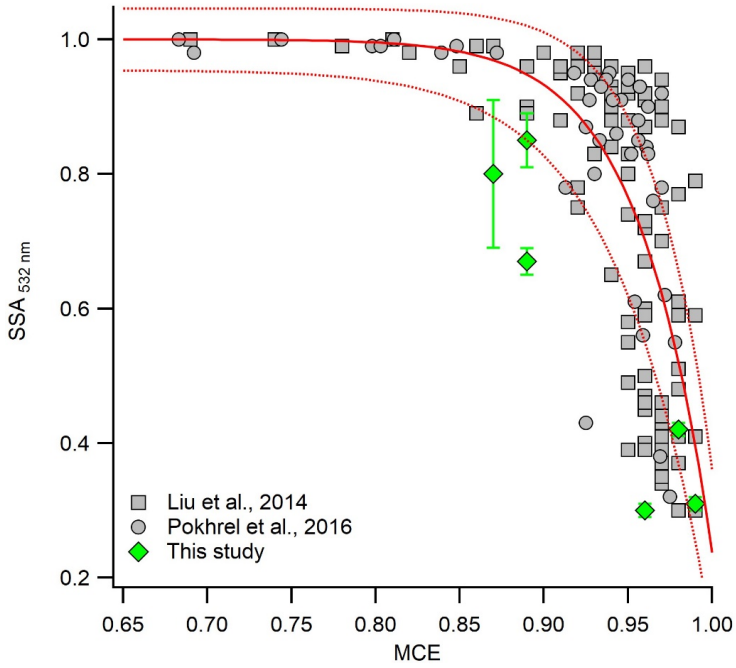

Figure 5: SSA of 400 nm size-selected aerosol at 532 nm as function of MCE under different combustion temperatures. Gray symbols are the SSA of bulk aerosol from previous studies (Liu et al., 2014; Pokhrel et al., 2016). Solid and dashed red lines are the best fit and the uncertainty bounds proposed by Liu et al. (2014).

3.4 Impact of dark aging on SSA

As BB aerosol ages, its properties evolve due to competing chemical and physical processes (Hodshire et al., 2019;Yokelson et al., 2009;Akagi et al., 2012;Vakkari et al., 2018;Formenti et al., 2003;Garofalo et al., 2019). The particle dynamics is different at night, compared to photochemical aging since there is a pronounced increase of particle size and density, which was also observed in previous laboratory and ambient measurements (Reid et al., 1998;Zhang et al., 2011). Even though the RH remains the same in our experiments, under high relative humidity conditions, heterogeneous reactions may be facilitated to produce more water soluble inorganic salts such as sulfates

Deleted: aerosol show consistent behavior as

Deleted: This outlier could also be because of the higher error associated with the error higher with the nephelometer, which is responsible for measuring scatteringscattering measured by the nephelometer. This could explain why our SSA calculations for BrC smoldering dominated aerosol was lower than expected.

Deleted: .

Deleted: For example, when acacia was burned at 500^{o} C, the SSA was 0.85 ± 0.04 for 400 nm size-selected aerosol, while at 800^{o} C, the SSA was 0.30 ± 0.01.

Deleted: (Liu et al., 2014).

Formatted: Font:10 pt

Formatted: Font:10 pt

Formatted: Pattern: Clear

Deleted: **5**:

Deleted:

Deleted: ... [4]

Deleted:

Deleted: ,

Deleted: The nighttime atmospheric processes are more complicated as dynamic changes in particle density and size may increase mass loading (Li et al., 2015).

Deleted: U

and nitrites (Shi et al., 2014). The first nighttime field analysis of BB plume intercepts for agricultural fuels showed that oxidation for rice straw and ponderosa pine was dominated by NO_3 (Decker et al., 2019). To simulate the impact of dark aging on aerosol optical properties, BB aerosol was aged without UV lights on and kept overnight for 24 hours. The relative humidity in these experiments was very low (i.e. below the detection limit of our instrument). Optical properties of the freshly emitted aerosol were measured initially, with repeat measurements taken after the particles were left in the chamber to age in the dark. Figure 6 shows the impact of dark aging on SSA for the 300 nm size-selected aerosol emitted during smoldering-dominated combustion. Regardless of fuel type, there occurred an increase in SSA during aging with some fuel dependence, the largest of which was observed for olive. A two-tail T-test confirmed that increase in mean SSA is statistically significant for all three cases. The results are similar for the 200 nm and 400 nm particles as shown in Table S1.

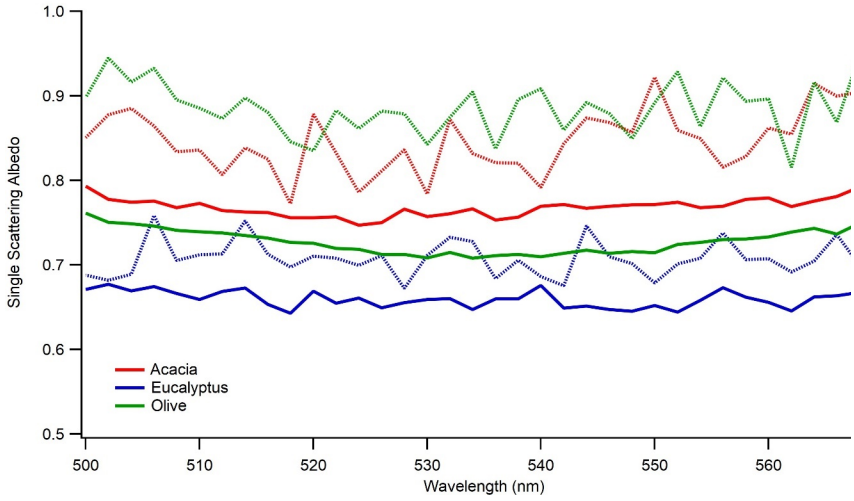

Figure 6: Impact of dark aging on SSA of 300 nm sized-selected aerosol emitted during smoldering-dominated combustion. Solid lines are for freshly emitted particle and dotted lines are for dark aged particles in the chamber. Different colors are for the different fuels listed in the legend.

Nighttime chemistry in BB studies is still unclear (Hodshire et al., 2019). The potential mechanism for the observed result could be due to nighttime oxidation initiated by ozone or nitrate chemistry or the formation of less/non-absorbing secondary organic aerosol. To further explore the possibility of the observed increase in SSA, we looked at the scattering and extinction cross-section of the fresh and dark aged aerosol. Figure S3 shows the changes in extinction and scattering cross-section of 300 nm size particles emitted during smoldering-dominated combustion under dark aging. For all fuel types studied, there occurred a significant increase in the scattering and extinction cross-section, indicating the occurrence of chemistry, even during dark aging. The increase in cross-section was driven by

Deleted:
Deleted:
Deleted: i
Deleted: The changes in optical properties is attributed to dark aging.
Deleted:
Deleted: 6
Deleted: -
Deleted: combustion at 500^{o}C
Deleted:
Deleted: 6:
Deleted: combustion at 500 oC
Formatted: Not Superscript/ Subscript
Deleted:
Deleted: .

the scattering cross-section, with no significant change in absorption cross-section during aging. If a greater portion of the particle consisted of scattering SOA, one would expect a decrease in absorption cross-section if scattering cross-section of the particle increase for a given particle size, but this does not seem to be the case. While we did not characterize the chemical constituents of dark aged BBA in these experiments, there is a significant body of literature that has. (Li et al., 2015;Ramasamy et al., 2019;Hartikainen et al., 2018) Previous work by Tiitta et al. (2016) investigated dark and UV aging under several combustion conditions. It is not entirely clear which is equivalent to our smoldering-dominated combustion cases, given that their "slow ignition" produced significantly more VOCs when compared to their "fast ignition" experiments, but more hydrocarbon-like POA was produced from "fast ignition" experiments. These experiments were not distinguished by a combustion temperature and the MCE was not measured, but they were differentiated based on the amount of kindling used in their masonry heater. In either case, a significant amount of organonitrates were formed during dark aging via oxidation from NO_3 in the presence of ozone. Only in the slow ignition case was there a significant formation of SOA from ozonolysis during dark aging (~12% by mass compared to ~12% from OH radical NO_3 and ~76% from and proxy radical). A significant increase in the inorganic fraction of the aerosol is not expected given the low RH in these experiments (Li et al., 2015). Hartikainen et al. (2018) also observed significant formation of nitrogen-containing organic compounds in both particulate and gas phase during dark aging, with significant partitioning into the condensed phase. Little oxidation of the particulate phase was observed compared to photochemical aging. While these studies examined chemical transformations in the particulate and gas phases, they did not characterize the effects of these changes on optical properties. Given the increase in the scattering cross-section of the particles without altering the absorption cross-section observed in this work, one likely explanation is that smaller particle with high fractions of BC increase their mobility diameter upon SOA formation. This SOA, however, is partially absorbing, so that the expected decrease in absorption is not seen; or is at least mitigated to a change within uncertainty. While this absorption must extend to the 500 – 570 nm region of the spectrum, several nitro-aromatic species and functionalized PAHs are able to absorb at such long wavelengths (Fleming et al., 2020).

Unlike smoldering-dominated combustion, we were not able to track the aging of aerosol emitted during flaming-dominated combustion due to some experimental issues. First, there was a significantly low aerosol emission due to more complete combustion of the fuel. For 300 nm and 400 nm size ranges, the number concentration of the particles emitted during flaming-dominated combustion was a factor of two to four lower than those emitted during smoldering-dominated combustion. In addition, due to the highly absorbing nature of the flaming- dominated aerosol, the scattering cross-section of the aerosol was significantly lower than that of the smoldering-dominated aerosol. Therefore, due to the very low number concentration and highly absorbing nature of the particles, the scattering coefficient of flaming-dominated aerosol was below the detection limit of our nephelometer during the aging experiments. Hence, we did not feel confident in reporting the SSA of dark aged particles emitted during flaming-dominated combustion. Figure S4 shows the impact of dark aging on the extinction cross-section of flaming-dominated aerosol. Even though a significant increase occurs in the extinction cross-sections during dark aging of smoldering-dominated aerosol, we did not observe such behaviors during aging of flaming-dominated aerosol, indicating no significant changes in their optical properties. As shown in Fig. S4 (b), there is a slight increase in the

Deleted: Nighttime chemistry in BB studies is still unclear (Hodshire et al., 2019). The potential mechanism for the observed result could be due to nighttime oxidation initiated by ozone or nitrate chemistry or the formation of less/non-absorbing secondary organic aerosol. To further explore the possibility of the observed increase in SSA, we looked at the scattering and extinction cross-section of the fresh and dark aged aerosol. Figure S2 shows the changes in extinction and scattering cross-section of 300 nm size particles emitted during combustion at 500° Csmoldering dominated combustion under dark aging. For all fuel types studied, there occurred a significant increase in the scattering and extinction cross-section, indicating the occurrence of chemistry, even during dark aging. The increase in cross-section was driven by the scattering cross-section, with no significant change in absorption cross-section during aging. This fact cannot be explained by the heterogeneous chemistry in aerosol phase when the particle size is selected, because one expects a decrease in absorption cross-section if scattering cross-section of the particle increases. Heterogeneous chemistry is common at high relative humidity (Shi et al., 2014). We hypothesized secondary organic aerosol formation as a potential phenomenon happening during dark aging. It was observed that dark aging produced higher amounts of nitrogen containing organ[... [5]

Deleted: the 500° C

Deleted:

Deleted: the

Deleted: 800° C

Deleted:

Deleted: at 800° C

Deleted:

Deleted: at 500° C

Deleted:

Deleted: emitted

Deleted: at 800° C

Deleted: those emitted at 500° C

Deleted:

Deleted: at 800° C

Deleted:

Deleted: combustion at 800° C

Deleted:

Deleted: 3

Deleted: at 800° C

Deleted: there occurs

Deleted: when combusted at 500° C

Deleted:

Deleted: combustion at 800° C

Deleted:

Deleted: the aerosol

Deleted: 3

extinction cross-section for olive. However, when accounting a 12 % uncertainty in the cross-section, this increase in extinction cross-section is statistically insignificant. Since the extinction cross-section does not change between fresh and dark aged BBA of the same aerosol, it can be inferred that there is no change in the SSA during dark aging of flaming-dominated aerosol. This could potentially be due to limited emission of the nighttime oxidants and VOCs, unlike during smoldering-dominated combustion.

3.5 Impact of photochemical aging

To study the impact of photochemical aging on the optical properties of aerosols, we performed the aging of BB aerosol with the UV lights turned on. In addition, to simulate the impact of photochemical aging in a polluted environment, we added VOCs (benzene, toluene, and xylene) to mimic urban pollution, as described in section 2.2.2. For both conditions, scattering and extinction coefficients were measured after 12 hours of aging in the chamber. Figure 7 shows the comparison of SSA from fresh and photochemically aged aerosols. As expected, there was an enhancement in the SSA of photochemically aged aerosol. A key point to mention is that fresh and aged SSA are from two different burns and we confirmed that under the same burn conditions the SSA of the same fuels remain within the measurement uncertainties of our instruments. Since this study used size-selected aerosols, the increase in SSA is only possible if the particles became less absorbing because of aging, which could potentially be due to the formation of non-absorbing secondary organic aerosol during photochemical aging. An increase in SSA is possible during photochemical aging due to degradation in brown carbon absorptivity (Sumlin et al., 2017), but the impact of brown carbon on SSA in mid-visible wavelength is small. BrC components undergo photochemical transformations during atmospheric transport, including photobleaching or photoenhancement of their absorption coefficients. For example, the field studies of Forrister et al. (2015) and Selimovic et al. (2018) observed a substantial decay in aerosol UV light absorption in biomass burning plumes corresponding to a half-life of 9 to 15 hours. Recent laboratory and field studies suggested that OH oxidation in the atmosphere may alter the optical properties of BrC, leading to absorption enhancement or bleaching (Schnitzler and Abbatt, 2018;Sumlin et al., 2017;Dasari et al., 2019). However, these studies were made at 375 and 405 nm wavelength of light, while ours were done in the visible range. As evident from Fig. 7, after 12 hours of aging, the BB aerosol becomes highly scattering, leading to SSA values of greater than 0.9 in the mid-visible wavelengths, even though fresh BB aerosol were highly absorbing, with SSA below 0.8.

Deleted: when combusted at 800° C

Deleted:

Deleted: when combusted at 500° C

Deleted:

Formatted: Indent: First line: 0"

Deleted: .

Formatted: Justified

Deleted: 1

Deleted: 7

Deleted: of

Deleted: occurred

Deleted:

Deleted: We attempted to study the impact of additional VOCs on SSA during aging. However, no distinct effect was observed. This is because we took our measurements after 12 hours of aging, which seems long enough to characterize the impact of the added VOC due to aging in UV. This fact suggests that a more carefully controlled study is needed to accurately simulate the impact of urban pollution on aerosol single scattering albedo.

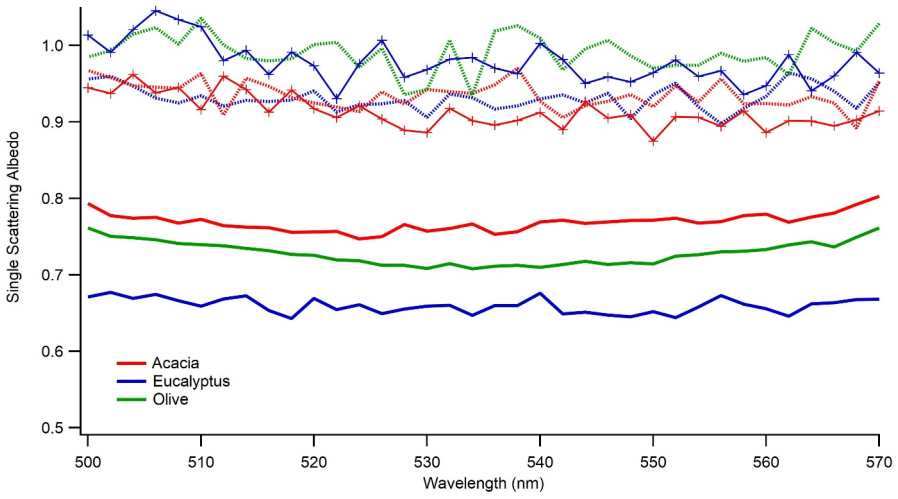

Figure 8: Impact of photochemical aging (light and light plus VOC) on SSA of 300 nm size-selected smoldering dominated aerosols. Solid lines are for freshly emitted particles, dotted lines are for aging under the light, and solid lines with symbols are for aging under light plus VOCs. Different colors are for the different fuels listed in the legend.

Despite the use of anthropogenic VOCs with concentrations larger than those average values found in urban and suburban regions of South Africa, no distinct effect was observed for SSA values of BB aerosol produced during smoldering-dominated combustion. This is most likely because we took our measurements after 12 hours of aging, which was enough time for the scattering nature of the SOA produced during aging to drive measured SSA values to unity, regardless of the chemical pathway taken due to the addition of VOCs. While it is possible that the relatively long aging time could obscure some of the effects due to the presence of VOCs, it is also possible that combustion products dominate molecular species, and the effects of additional VOCs are insignificant. The later would suggest that anthropogenic pollution does not seem to affect the optical properties of BB aerosol. Indeed, examining the effects of aging on the chemical composition of BB aerosol shows very few species that could be attributed to anthropogenic VOCs; specifically, only dihydroxyphthalic acid produced from xylene. For both Eucalyptus and Acacia, an isomer of dihydroxybenzene, such as resorcinol or catechol, was removed to the highest degree from the fresh BB aerosol upon photochemical aging. Generally, very few compounds were produced to a significant extent, and both fuels were dominated by a loss of chromatophoric lignin pyrolysis and distillation products. Not surprisingly, the associated absorbance from these chromophores, mostly from 200 – 350 nm, also attenuated with respect to age. This may be caused in part by the photo-bleaching effect created by the irradiation of UV light for 12 hours, heterogeneous OH oxidation, and SOA formation of non-chromophores.

This fact suggests that a study with higher temporal resolution is needed to simulate the impact of the VOCs on aerosol SSA, where continuous or much more frequent measurements are needed to determine the impact of urban

Deleted: 7:

Deleted: -

Deleted: d

Deleted:

Deleted: emitted at 500^{o} C combustion

Deleted: The impact of the VOCs can be studied by conducting continuous measurement, which is not possible for our setup when the size-selected mode is used. Like dark aged conditions, we were not able to estimate SSA for combustion at 800^{o}C due to the low particle concentration and highly absorbing nature of the aerosol.

Formatted: Indent: First line: 0"

Deleted:

Formatted: Font:Font color: Auto, Pattern: Clear

Comment [MNF25]: added

pollution on aerosol SSA. Such a study, using continuous measurements, is not possible for our setup when particles are also size selected. Like dark aged conditions, we were not able to estimate SSA for flaming dominated combustion due to the low particle concentration and highly absorbing nature of the aerosol. A chemical analysis of aged BB aerosol produced at this temperature revealed very few changes, suggesting that only a few molecular species are produced by combustion at this temperature.

During aging, the size distribution of the particles was measured every 5 minutes using an SMPS. To account for the impact of additional VOCs on secondary aerosol formation, we estimated the OA enhancement from the time series of SMPS spectra during these experiments. This was done by applying the constant wall loss rate constant as estimated in our previous study (Smith et al., 2019) and assuming a similar loss rate for POA vs SOA. We also assumed that OA is the major aerosol fraction emitted during smoldering-dominated combustion. In addition, we also made an assumption of constant density during aging, which gave us the lower estimate of the OA enhancement, because the density of the aerosol increases with age, compared to POA (Tkacik et al., 2017). The OA enhancement calculation method used in this study was based on the work by Saleh et al. (2013). Briefly, we applied the wall loss time constant to estimate the potential decrease in the OA mass loading only due to wall loss based on the OA mass before the lights were turned on. The OA enhancement factor was estimated by taking the ratio of measured aerosol mass to the predicted aerosol mass based on the wall loss rate constant. It is shown that partitioning of vapors to walls in laboratory experiments may alter apparent SOA production (Hodshire et al., 2019). For the particle wall loss rates used in this work, we did not correct for partitioning of vapors to walls, which was not generally negligible (Krechmer et al., 2016). Furthermore, it was shown that the tubing between the tube furnace and smog chamber might create loss in the gas phase precursors for SOA formation (Pagonis et al., 2017;Deming et al., 2019;Liu et al., 2019). Our connecting tubing was short enough (0.5 m) to neglect such a loss. Figure S5 shows the time series of OA enhancement during different aging conditions. We did not observe a distinct difference between the OA enhancement factors under light aged and light plus VOC aged cases. This could potentially be due to our assumptions and the uncertainty related to the SMPS. Previous field and modeling studies found significant enhancement in the SOA formation due to impact of urban pollution (Shrivastava et al., 2019). This fact also suggests that we need more rigorous study to simulate impact of urban pollution of secondary aerosol formation in the laboratory.

Although an ACSM was not available early in this study, we designed an experiment to compare the performance of the OA enhancement calculation based on the SMPS with the ACSM during a separate burn. As mentioned earlier, we used a first order decay of the POA based on the estimated wall loss rate constant from the chamber characterization experiments. Figure S6 shows the comparison of OA enhancement using the ACSM OA mass loading vs the estimated submicron aerosol mass based on the SMPS. In general, the trend of OA enhancement is similar, but the SMPS seems to underestimate the actual OA enhancement compared to the ACSM. The difference between the OA enhancement estimated by ACSM and SMPS is within 10 %, indicating that estimated OA enhancement lies within the SMPS uncertainty range.

4 Conclusions

Deleted: time series of

Deleted:

Deleted:

Deleted: at 500° C

Deleted: as the aerosol aged,

Deleted: aged

Deleted: as

Deleted: with

Deleted: Furthermore, it was shown that the tubing between the tube furnace and smog chamber might create loss and therefore delay the gas phase precursors for SOA formation (Pagonis et al., 2017;Deming et al., 2019;Liu et al., 2019). As described in section 2.1, in our set up, combustion emissions passed through a corrugated stainless steel transfer tube. Although relatively short (at 0.5 inches long), passage through this tube increased the loss of BB aerosol between the tube furnace and smog chamber due to the corrugated nature of the tubing. Significant cleaning of this corrugated tube was required between experiments, which indicated that the bulk of the losses between furnace and chamber occurred here. Figure S4 shows the time series of OA enhancement during different aging conditions. We did not observe a distinct difference between the OA enhancement factors under light aged and light plus VOC aged cases. This could potentially be due to our assumptions and the uncertainty related to the SMPS. Previous field and modeling studies found significant enhancement in the SOA formation due to impact of urban pollution (Shrivastava et al., 2019). This fact also suggests that we need more rigorous study to simulate impact of urban pollution of secondary aerosol formation in the laboratory.

Deleted: at a different time

Deleted: 5

Deleted: s

Biomass burning is the major source of atmospheric primary particles and vapors, which are precursors for secondary aerosols. BB aerosols have been extensively studied through both field and laboratory environments for North American fuels to understand the changes in optical and chemical properties as a function of aging. There is a clear research need for a wider sampling of fuels from different regions of the world for laboratory studies. This work is such an attempt to study the optical and chemical properties of fuels common in east Africa and represents the first such study.

The existence of significant variability in the observed field and laboratory measurements has been reviewed recently (Hodshire et al., 2019). While laboratory studies provide control over environmental and chemical conditions to study aging by controlling one variable at a time, it may not necessarily recreate atmospheric conditions in atmospheric plumes in the field. Differences in fuel mixture and fuel conditions, such as moisture content, can lead to different emissions. There is a difference in dilution rates between field studies, which is variable, and laboratory studies, which are not variable. Other differences include temperature differences, background OA concentrations, and wall losses. Despite the gap in reconciling field and laboratory studies, some limited comparisons can be made.

For fresh emissions, SSA showed no pronounced size dependence for flaming-dominated combustion, whereas same size dependence was observed for smoldering-dominated combustion. This may be due to the impact of multiply charged aerosol, which is not discriminated by the DMA. For the wavelength range used in this study, no wavelength dependence of SSA was observed under all conditions. However, SSA shows dependence on fuel type in general, even under the same combustion conditions.

In general, combustion temperature plays a major role in the optical properties of the emitted aerosol. In all cases the measured SSA values for flaming-dominated combustion are in the range between 0.287 to 0.439, indicating highly absorbing aerosol, which corresponds to aerosol dominated by black carbon. We observed a large increase in the SSA during smoldering-dominated combustion, which is in the range between 0.66 to 0.769. Under the same combustion conditions and airflow, there is a clear dependence of SSA on fuel type, with eucalyptus producing aerosol with higher SSA values than olive and acacia. However, these variations are relatively small, indicating that the SSA is more controlled by the combustion conditions than the fuel type.

Negative mode UPLC/DAD-ESI-HR-QTOFMS analyses of fresh BBA from flaming-dominated combustion suggest that there is some chemical constituent that is not being captured by this analysis. Given that Eucalyptus has a higher SSA than Acacia for the flaming-dominated combustion this would indicate that Eucalyptus has more non-absorbing OA that is not observed by chemical analysis, such as the presence of eucalyptol. Smoldering-dominate combustion of Eucalyptus and Acacia produced a variety of compounds in common, such as lignin pyrolysis products, distillation products, and cellulose breakdown products. Several lignin pyrolysis products and distillation products are more prevalent in Eucalyptus than in Acacia, while pyrolysis products of cellulose and at least one nitroaromatic species were more prevalent in Acacia. This is consistent with the higher SSA of Acacia when compared to Eucalyptus for the smoldering-dominated combustion, since lignin pyrolysis products and distillation products are known chromophores, while compounds derived from sugars and cellulose are non-chromophores.

Regardless of fuel types, there occurred an increase in SSA during dark aging, with some fuel dependence, the largest of which was observed for smoldering-dominated aerosol emitted from olive. A significant increase in the

scattering and extinction cross-section (mostly dominated by scattering) was observed, indicating the occurrence of chemistry, even during dark aging. Based on the relevant literature, we hypothesize that nitrogen-containing secondary organic aerosol is formed during dark aging (Li et al., 2015;Hartikainen et al., 2018;Nguyen et al., 2011;Tiitta et al., 2016) . It is possible that this SOA is absorbing in this region, which is offsetting the effect of an increasing OA fraction with age. A chemical analysis of dark aged aerosol during these experiments is planned for future work, and should allow us to test this theory.

After 12 hours of photochemical aging, BB aerosol becomes highly scattering with SSA values above 0.9, even though fresh emissions were more absorbing with SSA below 0.8. This can be attributed to oxidation in the chamber.

Due to the very low number concertation of flaming-dominated aerosols, the results were inconclusive, and we plan to conduct measurements by increasing the amount of fuel burned. We also attempted to simulate polluted urban environments by injecting anthropogenic VOCs into the chamber, but no distinct difference was observed. An examination of the chemical composition of aged BBA shows very few species that could be attributed to anthropogenic VOCs. Generally, very few compounds were produced to a significant extent, and both fuels were dominated by a loss of chromatophoric lignin pyrolysis and distillation products, likely caused by a combination of photo-bleaching, heterogeneous OH oxidation, and SOA formation of non-chromophores. No significant OA enhancement was observed because of the VOC injection either, even though significantly enhanced SOA formation was observed in polluted environments (Shrivastava et al., 2019;Shrivastava et al., 2015). This suggests a need for more rigorous controlled time dependent measurements.

To our knowledge, this is the first laboratory study of optical properties of east African biomass fuels for domestic use. Ongoing work includes systematic study of optical properties using six different African fuels as a function of aging, burn conditions, VOC concentration, and RH.

Author contribution: Damon Smith conducted the experiments and analyzed the data; Marc Fiddler and Solomon Bililign designed the experiments and contributed to writing and editing. Rudra Pokhrel contributed to the data analysis and interpretation.

Competing interests: The authors declare that they have no conflict of interest.

Deleted: Biomass burning is the major source of atmospheric primary particles and vapors, which are precursors for secondary aerosols. BB aerosols have been extensively studied through both field and laboratory environments for North American fuels to understand the changes in optical and chemical properties as a function of aging. There is a clear research need for a wider sampling of fuels from different regions of the world for laboratory studies. This work is such an attempt to study the optical and chemical properties of fuels common in east Africa and represents the first such study. ... [6]

Deleted:

References

Akagi, S. K., Craven, J. S., Taylor, J. W., McMeeking, G. R., Yokelson, R. J., Burling, I. R., Urbanski, S. P., Wold, C. E., Seinfeld, J. H., Coe, H., Alvarado, M. J., and Weise, D. R.: Evolution of trace gases and particles emitted by a chaparral fire in California, Atmos. Chem. Phys., 12, 1397-1421, 10.5194/acp-12-1397-2012, 2012.

Andreae, M. O., and Merlet, P.: Emission of trace gases and aerosols from biomass burning, Global Biogeochemical Cycles, 15, 955-966, 10.1029/2000GB001382, 2001.

Babar, Z. B., Park, J.-H., Kang, J., and Lim, H.-J.: Characterization of a Smog Chamber for Studying Formation and Physicochemical Properties of Secondary Organic Aerosol, Aerosol and Air Quality Research, 16, 3102-3113, 10.4209/aaqr.2015.10.0580, 2016.

Bahadur, R., Praveen, P. S., Xu, Y., and Ramanathan, V.: Solar absorption by elemental and brown carbon determined from spectral observations, Proceedings of the National Academy of Sciences, 109, 17366-17371, 10.1073/pnas.1205910109, 2012.

Bank, W.: More People Have Access to Electricity Than Ever Before, but World Is Falling Short of Sustainable Energy Goals, in, 2019.

Bond, T. C., Anderson, T. L., and Campbell, D.: Calibration and intercomparison of filter-based measurements of visible light absorption by aerosols, Aerosol Science and Technology, 30, 582-600, 10.1080/027868299304435, 1999.

Bond, T. C., Streets, D. G., Yarber, K. F., Nelson, S. M., Woo, J.-H., and Klimont, Z.: A technology-based global inventory of black and organic carbon emissions from combustion, Journal of Geophysical Research: Atmospheres, 109, n/a-n/a, 10.1029/2003JD003697, 2004.

Bond, T. C., Bhardwaj, E., Dong, R., Jogani, R., Jung, S., Roden, C., Streets, D. G., and Trautmann, N. M.: Historical emissions of black and organic carbon aerosol from energy-related combustion, 1850–2000, Global Biogeochemical Cycles, 21, n/a-n/a, 10.1029/2006GB002840, 2007.

Bond, T. C., Zarzycki, C., Flanner, M. G., and Koch, D. M.: Quantifying immediate radiative forcing by black carbon and organic matter with the Specific Forcing Pulse, Atmos. Chem. Phys., 11, 1505-1525, 10.5194/acp-11-1505-2011, 2011.

Boucher, O., D. Randall, P. Artaxo, C. Bretherton, G. Feingold, P. Forster, V.-M. Kerminen, Y. Kondo, H. Liao, U. Lohmann, P. Rasch, S.K. Satheesh, S. Sherwood, B. Stevens and X.Y. Zhang:

Clouds and Aerosols, in: Climate Change 2013: The Physical Science Basis. Contribution of Working Group I to the Fifth Assessment Report of the Intergovernmental Panel on Climate Change, edited by: Stocker, T. F., D. Qin, G.-K. Plattner, M. Tignor, S.K. Allen, J. Boschung, A. Nauels, Y. Xia, V. Bex and P.M. Midgley Cambridge University Press, Cambridge, United Kingdom and New York, NY, USA., 2013.
Brown, H., Liu, X., Feng, Y., Jiang, Y., Wu, M., Lu, Z., Wu, C., Murphy, S., and Pokhrel, R.: Radiative effect and climate impacts of brown carbon with the Community Atmosphere Model (CAM5), Atmos. Chem. Phys., 18, 17745-17768, 10.5194/acp-18-17745-2018, 2018.
Bruns, E. A., El Haddad, I., Slowik, J. G., Kilic, D., Klein, F., Baltensperger, U., and Prévôt, A. S. H.: Identification of significant precursor gases of secondary organic aerosols from residential wood combustion, Scientific Reports, 6, 27881, 10.1038/srep27881 https://www.nature.com/articles/srep27881 - supplementary-information, 2016.
Christian, T. J., Kleiss, B., Yokelson, R. J., Holzinger, R., Crutzen, P. J., Hao, W. M., Saharjo, B. H., and Ward, D. E.: Comprehensive laboratory measurements of biomass-burning emissions: 1. Emissions from Indonesian, African, and other fuels, Journal of Geophysical Research-Atmospheres, 108, 10.1029/2003jd003704, 2003.
Chung, C. E., Ramanathan, V., and Decremer, D.: Observationally constrained estimates of carbonaceous aerosol radiative forcing, Proceedings of the National Academy of Sciences, 109, 11624-11629, 10.1073/pnas.1203707109, 2012.
Crutzen, P., and Andreae, M.: Biomass Burning in the Tropics: Impact on Atmospheric Chemistry and Biogeochemical Cycles, Science (New York, N.Y.), 250, 1669-1678, 10.1126/science.250.4988.1669, 1991.
Dasari, S., Andersson, A., Bikkina, S., Holmstrand, H., Budhavant, K., Satheesh, S., Asmi, E., Kesti, J., Backman, J., Salam, A., Bisht, D. S., Tiwari, S., Hameed, Z., and Gustafsson, Ö.: Photochemical degradation affects the light absorption of water-soluble brown carbon in the South Asian outflow, Science Advances, 5, eaau8066, 10.1126/sciadv.aau8066, 2019.
Decker, Z. C. J., Zarzana, K. J., Coggon, M., Min, K.-E., Pollack, I., Ryerson, T. B., Peischl, J., Edwards, P., Dubé, W. P., Markovic, M. Z., Roberts, J. M., Veres, P. R., Graus, M., Warneke, C., de Gouw, J., Hatch, L. E., Barsanti, K. C., and Brown, S. S.: Nighttime Chemical Transformation in Biomass Burning Plumes: A Box Model Analysis Initialized with Aircraft Observations, Environmental Science & Technology, 53, 2529-2538, 10.1021/acs.est.8b05359, 2019.
Delfino, R. J., Brummel, S., Wu, J., Stern, H., Ostro, B., Lipsett, M., Winer, A., Street, D. H., Zhang, L., Tjoa, T., and Gillen, D. L.: The relationship of respiratory and cardiovascular hospital admissions to the southern California wildfires of 2003, Occupational and Environmental Medicine, 66, 189-197, 10.1136/oem.2008.041376, 2009.
Deming, B. L., Pagonis, D., Liu, X., Day, D. A., Talukdar, R., Krechmer, J. E., Gouw, J. A. d., Jimenez, J. L., and Ziemann, P. J.: Measurements of Delays of Gas-Phase Compounds in a Wide Variety of Tubing Materials due to Gas–wall Interactions, Atmos. Meas. Tech., 12, 3453, 2019.
Eck, T. F., Holben, B. N., Ward, D. E., Dubovik, O., Reid, J. S., Smirnov, A., Mukelabai, M. M., Hsu, N. C., O'Neill, N. T., and Slutsker, I.: Characterization of the optical properties of biomass burning aerosols in Zambia during the 1997 ZIBBEE field campaign, Journal of Geophysical Research: Atmospheres, 106, 3425-3448, 10.1029/2000JD900555, 2001.
Edwards, D. P., Emmons, L. K., Gille, J. C., Chu, A., Attié, J. L., Giglio, L., Wood, S. W., Haywood, J., Deeter, M. N., Massie, S. T., Ziskin, D. C., and Drummond, J. R.: Satellite-observed pollution

from Southern Hemisphere biomass burning, Journal of Geophysical Research: Atmospheres, 111, n/a-n/a, 10.1029/2005JD006655, 2006.
Elliott, C. T., Henderson, S. B., and Wan, V.: Time series analysis of fine particulate matter and asthma reliever dispensations in populations affected by forest fires, Environmental Health, 12, 11, 10.1186/1476-069X-12-11, 2013.
Feng, Y., Ramanathan, V., and Kotamarthi, V.: Brown carbon: A significant atmospheric absorber of solar radiation, ATMOSPHERIC CHEMISTRY AND PHYSICS, 13, 8607-8621, 10.5194/acp-13-8607-2013, 2013.
Formenti, P., Elbert, W., Maenhaut, W., Haywood, J., Osborne, S., and Andreae, M.: Inorganic and carbonaceous aerosols during the Southern African Regional Science Initiative (SAFARI 2000) experiment: Chemical characteristics, physical properties, and emission data for smoke from African biomass burning, Journal of Geophysical Research: Atmospheres, 108, https://doi.org/10.1029/2002jd002408, 2003.
Forrister, H., Liu, J., Scheuer, E., Dibb, J., Ziemba, L., Thornhill, K. L., Anderson, B., Diskin, G., Perring, A. E., and Schwarz, J. P.: Evolution of Brown Carbon in Wildfire Plumes, Geophys. Res. Lett., 42, 4623, 2015.
Forster, P., Ramaswamy, V., Artaxo, P., Berntsen, T., Betts, R., Fahey, D., Haywood, J., Lean, J., Lowe, D., Myhre, G., Nganga, J., Prinn, R., Raga, G., Schulz, M., Dorland, R., Bodeker, G., Boucher, O., Collins, W., Conway, T., and Whorf, T.: Changes in Atmospheric Constituents and in Radiative Forcing, in, 2007.
Garofalo, L. A., Pothier, M. A., Levin, E. J. T., Campos, T., Kreidenweis, S. M., and Farmer, D. K.: Emission and Evolution of Submicron Organic Aerosol in Smoke from Wildfires in the Western United States, ACS Earth Space Chem., 3, 1237, 2019.
Hartikainen, A., Yli-Pirilä, P., Tiitta, P., Leskinen, A., Kortelainen, M., Orasche, J., Schnelle-Kreis, J., Lehtinen, K. E. J., Zimmermann, R., Jokiniemi, J., and Sippula, O.: Volatile Organic Compounds from Logwood Combustion: Emissions and Transformation under Dark and Photochemical Aging Conditions in a Smog Chamber, Environmental Science & Technology, 52, 4979-4988, 10.1021/acs.est.7b06269, 2018.
Henderson, S. B., Brauer, M., MacNab, Y. C., and Kennedy, S. M.: Three Measures of Forest Fire Smoke Exposure and Their Associations with Respiratory and Cardiovascular Health Outcomes in a Population-Based Cohort, Environmental Health Perspectives, 119, 1266-1271, doi:10.1289/ehp.1002288, 2011.
Hennigan, C. J., Miracolo, M. A., Engelhart, G. J., May, A. A., Presto, A. A., Lee, T., Sullivan, A. P., McMeeking, G. R., Coe, H., Wold, C. E., Hao, W. M., Gilman, J. B., Kuster, W. C., de Gouw, J., Schichtel, B. A., Collett Jr, J. L., Kreidenweis, S. M., and Robinson, A. L.: Chemical and physical transformations of organic aerosol from the photo-oxidation of open biomass burning emissions in an environmental chamber, Atmos. Chem. Phys., 11, 7669-7686, 10.5194/acp-11-7669-2011, 2011.
Hodshire, A. L., Akherati, A., Alvarado, M. J., Brown-Steiner, B., Jathar, S. H., Jimenez, J. L., Kreidenweis, S. M., Lonsdale, C. R., Onasch, T. B., Ortega, A. M., and Pierce, J. R.: Aging Effects on Biomass Burning Aerosol Mass and Composition: A Critical Review of Field and Laboratory Studies, Environmental Science & Technology, 53, 10007-10022, 10.1021/acs.est.9b02588, 2019.

Hodzic, A., Madronich, S., Bohn, B., Massie, S., Menut, L., and Wiedinmyer, C.: Wildfire particulate matter in Europe during summer 2003: meso-scale modeling of smoke emissions, transport and radiative effects, Atmos. Chem. Phys., 7, 4043-4064, 10.5194/acp-7-4043-2007, 2007.
Holstius, D. M., Reid, C. E., Jesdale, B. M., and Morello-Frosch, R.: Birth Weight following Pregnancy during the 2003 Southern California Wildfires, Environmental Health Perspectives, 120, 1340-1345, doi:10.1289/ehp.1104515, 2012.
Hungershoefer, K., Zeromskiene, K., Iinuma, Y., Helas, G., Trentmann, J., Trautmann, T., Parmar, R., Wiedensohler, A., Andreae, M., and Schmid, O.: Modelling the optical properties of fresh biomass burning aerosol produced in a smoke chamber: results from the EFEU campaign, Atmospheric Chemistry and Physics, 8, 3427-3439, https://doi.org/10.5194/acp-8-3427-2008, 2008.
Ichoku, C., Giglio, L., Wooster, M. J., and Remer, L. A.: Global characterization of biomass-burning patterns using satellite measurements of fire radiative energy, Remote Sensing of Environment, 112, 2950-2962, https://doi.org/10.1016/j.rse.2008.02.009, 2008.
IPCC: IPCC Fifth Assessment Report, Climate Change 2013: The Physical Science Basis, 2014.
Jacobson, M. Z.: A physically-based treatment of elemental carbon optics: Implications for global direct forcing of aerosols, Geophysical Research Letters, 27, 217-220, 10.1029/1999GL010968, 2000.
Johnston, F., Hanigan, I., Henderson, S., Morgan, G., and Bowman, D.: Extreme air pollution events from bushfires and dust storms and their association with mortality in Sydney, Australia 1994–2007, Environmental Research, 111, 811-816, https://doi.org/10.1016/j.envres.2011.05.007, 2011.
Johnston, F. H., Henderson, S. B., Chen, Y., Randerson, J. T., Marlier, M., DeFries, R. S., Kinney, P., Bowman, D. M. J. S., and Brauer, M.: Estimated Global Mortality Attributable to Smoke from Landscape Fires, Environmental Health Perspectives, 120, 695-701, doi:10.1289/ehp.1104422, 2012.
Kirchstetter, T. W., Novakov, T., and Hobbs, P. V.: Evidence that the spectral dependence of light absorption by aerosols is affected by organic carbon, Journal of Geophysical Research: Atmospheres, 109, doi:10.1029/2004JD004999, 2004.
Klimont, Z., Cofala, J., Xing, J., Wei, W., Zhang, C., Wang, S., Kejun, J., Bhandari, P., Mathur, R., Purohit, P., Rafaj, P., Chambers, A., Amann, M., and Hao, J.: Projections of SO2, NOx and carbonaceous aerosols emissions in Asia, Tellus B, 61, 602-617, 10.1111/j.1600-0889.2009.00428.x, 2009.
Klimont, Z., Smith, S. J., and Cofala, J.: The last decade of global anthropogenic sulfur dioxide: 2000–2011 emissions, Environmental Research Letters, 8, 014003, 2013.
Koch, D., Menon, S., Genio, A. D., Ruedy, R., Alienov, I., and Schmidt, G. A.: Distinguishing Aerosol Impacts on Climate over the Past Century, Journal of Climate, 22, 2659-2677, 10.1175/2008jcli2573.1, 2009.
Krechmer, J. E., Pagonis, D., Ziemann, P. J., and Jimenez, J. L.: Quantification of Gas-Wall Partitioning in Teflon Environmental Chambers Using Rapid Bursts of Low-Volatility Oxidized Species Generated in Situ, Environ. Sci. Technol., 50, 5757, 2016.
Lamarque, J. F., Bond, T. C., Eyring, V., Granier, C., Heil, A., Klimont, Z., Lee, D., Liousse, C., Mieville, A., Owen, B., Schultz, M. G., Shindell, D., Smith, S. J., Stehfest, E., Van Aardenne, J.,

Cooper, O. R., Kainuma, M., Mahowald, N., McConnell, J. R., Naik, V., Riahi, K., and van Vuuren, D. P.: Historical (1850–2000) gridded anthropogenic and biomass burning emissions of reactive gases and aerosols: methodology and application, Atmos. Chem. Phys., 10, 7017-7039, 10.5194/acp-10-7017-2010, 2010.
Laskin, A., Laskin, J., and Nizkorodov, S. A.: Chemistry of Atmospheric Brown Carbon, Chemical Reviews, 115, 4335-4382, 10.1021/cr5006167, 2015.
Leskinen, A., Yli-Pirilä, P., Kuuspalo, K., Sippula, O., Jalava, P., Hirvonen, M. R., Jokiniemi, J., Virtanen, A., Komppula, M., and Lehtinen, K. E. J.: Characterization and testing of a new environmental chamber, Atmos. Meas. Tech., 8, 2267-2278, 10.5194/amt-8-2267-2015, 2015.
Levin, E. J. T., McMeeking, G. R., Carrico, C. M., Mack, L. E., Kreidenweis, S. M., Wold, C. E., Moosmüller, H., Arnott, W. P., Hao, W. M., Collett, J. L., and Malm, W. C.: Biomass burning smoke aerosol properties measured during Fire Laboratory at Missoula Experiments (FLAME), Journal of Geophysical Research: Atmospheres, 115, D18210, 10.1029/2009JD013601, 2010.
Li, C., Ma, Z., Chen, J., Wang, X., Ye, X., Wang, L., Yang, X., Kan, H., Donaldson, D. J., and Mellouki, A.: Evolution of biomass burning smoke particles in the dark, Atmospheric Environment, 120, 244-252, https://doi.org/10.1016/j.atmosenv.2015.09.003, 2015.
Liousse, C., Guillaume, B., Grégoire, J. M., Mallet, M., Galy, C., Pont, V., Akpo, A., Bedou, M., Castéra, P., Dungall, L., Gardrat, E., Granier, C., Konaré, A., Malavelle, F., Mariscal, A., Mieville, A., Rosset, R., Serça, D., Solmon, F., Tummon, F., Assamoi, E., Yoboué, V., and Van Velthoven, P.: Updated African biomass burning emission inventories in the framework of the AMMA-IDAF program, with an evaluation of combustion aerosols, Atmos. Chem. Phys., 10, 9631-9646, 10.5194/acp-10-9631-2010, 2010.
Liousse, C., Assamoi, E., Criqui, P., Granier, C., and Rosset, R.: Explosive growth in African combustion emissions from 2005 to 2030, Environmental Research Letters, 9, 035003, https://doi.org/10.1088/1748-9326/9/3/035003, 2014.
Liu, S., Aiken, A. C., Arata, C., Dubey, M. K., Stockwell, C. E., Yokelson, R. J., Stone, E. A., Jayarathne, T., Robinson, A. L., DeMott, P. J., and Kreidenweis, S. M.: Aerosol single scattering albedo dependence on biomass combustion efficiency: Laboratory and field studies, Geophysical Research Letters, 41, 742-748, 10.1002/2013GL058392, 2014.
Liu, X., Huey, L. G., Yokelson, R. J., Selimovic, V., Simpson, I. J., Müller, M., Jimenez, J. L., Campuzano-Jost, P., Beyersdorf, A. J., and Blake, D. R.: Airborne Measurements of Western US Wildfire Emissions: Comparison with Prescribed Burning and Air Quality Implications, J. Geophys. Res. D: Atmos., 122, 6108, 2017.
Liu, X., Deming, B., Pagonis, D., Day, D. A., Palm, B. B., Talukdar, R., Roberts, J. M., Veres, P. R., Krechmer, J. E., Thornton, J. A., de Gouw, J. A., Ziemann, P. J., and Jimenez, J. L.: Effects of gas–wall interactions on measurements of semivolatile compounds and small polar molecules, Atmos. Meas. Tech., 12, 3137-3149, 10.5194/amt-12-3137-2019, 2019.
Ma, X., Yu, F., and Luo, G.: Aerosol direct radiative forcing based on GEOS-Chem-APM and uncertainties, Atmos. Chem. Phys., 12, 5563-5581, 10.5194/acp-12-5563-2012, 2012.
Mack, L. A., Levin, E. J. T., Kreidenweis, S. M., Obrist, D., Moosmüller, H., Lewis, K. A., Arnott, W. P., McMeeking, G. R., Sullivan, A. P., Wold, C. E., Hao, W. M., Collett Jr, J. L., and Malm, W. C.: Optical closure experiments for biomass smoke aerosols, Atmos. Chem. Phys., 10, 9017-9026, 10.5194/acp-10-9017-2010, 2010.

Mack, L. E.: Cavity Ring-Down Sectroscopy and the Retrieval of Aerosol Optical Properties from Biomass Burning During Flame 2, Master's, Colorado State University, CO, USA, 2008.
Malavelle, F., Pont, V., Mallet, M., Solmon, F., Johnson, B., Leon, J.-F., and Liousse, C.: Simulation of aerosol radiative effects over West Africa during DABEX and AMMA SOP-0, Journal of Geophysical Research: Atmospheres, 116, n/a-n/a, 10.1029/2010JD014829, 2011.
McMeeking, G. R., Kreidenweis, S. M., Baker, S., Carrico, C. M., Chow, J. C., Collett, J. L., Hao, W. M., Holden, A. S., Kirchstetter, T. W., Malm, W. C., Moosmüller, H., Sullivan, A. P., and Wold, C. E.: Emissions of trace gases and aerosols during the open combustion of biomass in the laboratory, Journal of Geophysical Research: Atmospheres, 114, D19210, 10.1029/2009JD011836, 2009.
Miles, R. E. H., Rudić, S., Orr-Ewing, A. J., and Reid, J. P.: Sources of Error and Uncertainty in the Use of Cavity Ring Down Spectroscopy to Measure Aerosol Optical Properties, Aerosol Science and Technology, 45, 1360-1375, 10.1080/02786826.2011.596170, 2011.
Moosmüller, H., Varma, R., and Arnott, W. P.: Cavity Ring-Down and Cavity-Enhanced Detection Techniques for the Measurement of Aerosol Extinction, Aerosol Science and Technology, 39, 30-39, 10.1080/027868290903880, 2005.
Naeher, L. P., Brauer, M., Lipsett, M., Zelikoff, J. T., Simpson, C. D., Koenig, J. Q., and Smith, K. R.: Woodsmoke Health Effects: A Review, Inhalation Toxicology, 19, 67-106, 10.1080/08958370600985875, 2007.
Ng, N. L., Herndon, S. C., Trimborn, A., Canagaratna, M. R., Croteau, P. L., Onasch, T. B., Sueper, D., Worsnop, D. R., Zhang, Q., Sun, Y. L., and Jayne, J. T.: An Aerosol Chemical Speciation Monitor (ACSM) for Routine Monitoring of the Composition and Mass Concentrations of Ambient Aerosol, Aerosol Science and Technology, 45, 780-794, 10.1080/02786826.2011.560211, 2011.
Pagonis, D., Krechmer, J. E., Gouw, J., Jimenez, J. L., and Ziemann, P. J.: Effects of Gas–wall Partitioning in Teflon Tubing and Instrumentation on Time-Resolved Measurements of Gas-Phase Organic Compounds, Atmos. Meas. Tech., 10, 4687, 2017.
Paulsen, D., Dommen, J., Kalberer, M., Prévôt, A. S. H., Richter, R., Sax, M., Steinbacher, M., Weingartner, E., and Baltensperger, U.: Secondary Organic Aerosol Formation by Irradiation of 1,3,5-Trimethylbenzene−NOx−H2O in a New Reaction Chamber for Atmospheric Chemistry and Physics, Environmental Science & Technology, 39, 2668-2678, 10.1021/es0489137, 2005.
Pokhrel, R. P., Wagner, N. L., Langridge, J. M., Lack, D. A., Jayarathne, T., Stone, E. A., Stockwell, C. E., Yokelson, R. J., and Murphy, S. M.: Parameterization of single-scattering albedo (SSA) and absorption Ångström exponent (AAE) with EC / OC for aerosol emissions from biomass burning, Atmos. Chem. Phys., 16, 9549-9561, 10.5194/acp-16-9549-2016, 2016.
Poudel, S., Fiddler, M., Smith, D., Flurchick, K., and Bililign, S.: Optical properties of biomass burning aerosols: Comparison of experimental measurements and T-Matrix calculations, Atmosphere, 8, 228, https://doi.org/10.3390/atmos8110228, 2017.
Radney, J. G., Bazargan, M. H., Wright, M. E., and Atkinson, D. B.: Laboratory Validation of Aerosol Extinction Coefficient Measurements by a Field-Deployable Pulsed Cavity Ring-Down Transmissometer, Aerosol Science and Technology, 43, 71-80, 10.1080/02786820802482536, 2009.
Radney, J. G., Ma, X., Gillis, K. A., Zachariah, M. R., Hodges, J. T., and Zangmeister, C. D.: Anal. Chem., 85, 8319, 2013.

Ramasamy, S., Nakayama, T., Imamura, T., Morino, Y., Kajii, Y., and Sato, K.: Investigation of dark condition nitrate radical- and ozone-initiated aging of toluene secondary organic aerosol: Importance of nitrate radical reactions with phenolic products, Atmospheric Environment, 219, 117049, https://doi.org/10.1016/j.atmosenv.2019.117049, 2019.
Rappold, A. G., Stone, S. L., Cascio, W. E., Neas, L. M., Kilaru, V. J., Carraway, M. S., Szykman, J. J., Ising, A., Cleve, W. E., Meredith, J. T., Vaughan-Batten, H., Deyneka, L., and Devlin, R. B.: Peat Bog Wildfire Smoke Exposure in Rural North Carolina Is Associated with Cardiopulmonary Emergency Department Visits Assessed through Syndromic Surveillance, Environmental Health Perspectives, 119, 1415-1420, doi:10.1289/ehp.1003206, 2011.
Reid, J. S., Hobbs, P. V., Ferek, R. J., Blake, D. R., Martins, J. V., Dunlap, M. R., and Liousse, C.: Physical, Chemical, and Optical Properties of Regional Hazes Dominated by Smoke in Brazil, J. Geophys. Res., 103, 32059, 1998.
Roberts, G., Wooster, M. J., and Lagoudakis, E.: Annual and diurnal african biomass burning temporal dynamics, Biogeosciences, 6, 849-866, 10.5194/bg-6-849-2009, 2009.
Roberts, G. J., and Wooster, M. J.: Fire Detection and Fire Characterization Over Africa Using Meteosat SEVIRI, IEEE Transactions on Geoscience and Remote Sensing, 46, 1200-1218, 10.1109/TGRS.2008.915751, 2008.
Saleh, R., Robinson, E. S., Tkacik, D. S., Ahern, A. T., Liu, S., Aiken, A. C., Sullivan, R. C., Presto, A. A., Dubey, M. K., Yokelson, R. J., Donahue, N. M., and Robinson, A. L.: Brownness of organics in aerosols from biomass burning linked to their black carbon content, Nature Geoscience, 7, 647-650, 10.1038/ngeo2220, 2014.
Saleh, R., Marks, M., Heo, J., Adams, P. J., Donahue, N. M., and Robinson, A. L.: Contribution of brown carbon and lensing to the direct radiative effect of carbonaceous aerosols from biomass and biofuel burning emissions, Journal of Geophysical Research: Atmospheres, 120, 10,285-210,296, 10.1002/2015jd023697, 2015.
Saleh, R., Cheng, Z., and Atwi, K.: The Brown–Black Continuum of Light-Absorbing Combustion Aerosols, Environmental Science & Technology Letters, 5, 508-513, 10.1021/acs.estlett.8b00305, 2018.
Schnitzler, E. G., and Abbatt, J. P. D.: Heterogeneous OH oxidation of secondary brown carbon aerosol, Atmos. Chem. Phys., 18, 14539-14553, 10.5194/acp-18-14539-2018, 2018.
Schultz, M. G., Heil, A., Hoelzemann, J. J., Spessa, A., Thonicke, K., Goldammer, J. G., Held, A. C., Pereira, J. M. C., and van het Bolscher, M.: Global wildland fire emissions from 1960 to 2000, Global Biogeochemical Cycles, 22, GB2002, 10.1029/2007GB003031, 2008.
Schwarz, J. P., Spackman, J. R., Fahey, D. W., Gao, R. S., Lohmann, U., Stier, P., Watts, L. A., Thomson, D. S., Lack, D. A., Pfister, L., Mahoney, M. J., Baumgardner, D., Wilson, J. C., and Reeves, J. M.: Coatings and their enhancement of black carbon light absorption in the tropical atmosphere, Journal of Geophysical Research: Atmospheres, 113, n/a-n/a, 10.1029/2007JD009042, 2008.
Selimovic, V., Yokelson, R. J., Warneke, C., Roberts, J. M., Gouw, J., Reardon, J., and Griffith, D. W. T.: Aerosol Optical Properties and Trace Gas Emissions by PAX and OP-FTIR for Laboratory-Simulated Western US Wildfires during FIREX, Atmos. Chem. Phys., 18, 2929, 2018.
Sheridan, P. J., Arnott, W. P., Ogren, J. A., Andrews, E., Atkinson, D. B., Covert, D. S., Moosmuller, H., Petzold, A., Schmid, B., Strawa, A. W., Varma, R., and Virkkula, A.: The Reno

Aerosol Optics Study: An evaluation of aerosol absorption measurement methods, Aerosol Science and Technology, 39, 1-16, 10.1080/027868290901891, 2005.
Shi, Y., Chen, J., Hu, D., Wang, L., Yang, X., and Wang, X.: Airborne submicron particulate (PM1) pollution in Shanghai, China: Chemical variability, formation/dissociation of associated semi-volatile components and the impacts on visibility, Science of The Total Environment, 473-474, 199-206, https://doi.org/10.1016/j.scitotenv.2013.12.024, 2014.
Shrivastava, M., Andreae, M. O., Artaxo, P., Barbosa, H. M. J., Berg, L. K., Brito, J., Ching, J., Easter, R. C., Fan, J., Fast, J. D., Feng, Z., Fuentes, J. D., Glasius, M., Goldstein, A. H., Alves, E. G., Gomes, H., Gu, D., Guenther, A., Jathar, S. H., Kim, S., Liu, Y., Lou, S., Martin, S. T., McNeill, V. F., Medeiros, A., de Sá, S. S., Shilling, J. E., Springston, S. R., Souza, R. A. F., Thornton, J. A., Isaacman-VanWertz, G., Yee, L. D., Ynoue, R., Zaveri, R. A., Zelenyuk, A., and Zhao, C.: Urban pollution greatly enhances formation of natural aerosols over the Amazon rainforest, Nature Communications, 10, 1046, 10.1038/s41467-019-08909-4, 2019.
Singh, S., Fiddler, M. N., Smith, D., and Bililign, S.: Error analysis and uncertainty in the determination of aerosol optical properties using cavity ring-down spectroscopy, integrating nephelometry, and the extinction-minus-scattering method, Aerosol Science and Technology, 48, 1345-1359, https://doi.org/10.1080/02786826.2014.984062, 2014.
Singh, S., Fiddler, M. N., and Bililign, S.: Measurement of size-dependent single scattering albedo of fresh biomass burning aerosols using the extinction-minus-scattering technique with a combination of cavity ring-down spectroscopy and nephelometry, Atmos. Chem. Phys., 16, 13491-13507, 10.5194/acp-16-13491-2016, 2016.
Smith, D. M., Fiddler, M. N., Sexton, K. G., and Bililign, S.: Construction and Characterization of an Indoor Smog Chamber for Measuring the Optical and Physicochemical Properties of Aging Biomass Burning Aerosols, Aerosol and Air Quality Research, 19, 467-483, 10.4209/aaqr.2018.06.0243, 2019.
Smith, D. M., Cui, T., Fiddler, M. N., Pokhrel, R., Surratt, J. D., and Bililign, S.: Laboratory studies of fresh and aged biomass burning aerosols emitted from east African biomass fuels - Part 2: Chemical properties and characterization, Atmos. Chem. Phys. Discuss., 2020, 1-30, 10.5194/acp-2019-1160, 2020.
Smith, K. R., and Pillarisetti, A.: Household Air Pollution from Solid Cookfuels and Its Effects on Health., in: Injury Prevention and Environmental Health. 3rd edition, edited by: CN, M., Nugent R, and O, K., The International Bank for Reconstruction and Development / The World Bank;, Washington (DC), 2017.
Spracklen, D. V., Mickley, L. J., Logan, J. A., Hudman, R. C., Yevich, R., Flannigan, M. D., and Westerling, A. L.: Impacts of climate change from 2000 to 2050 on wildfire activity and carbonaceous aerosol concentrations in the western United States, Journal of Geophysical Research: Atmospheres, 114, 10.1029/2008jd010966, 2009.
Stefanidou, M., Athanaselis, S., and Spiliopoulou, C.: Health Impacts of Fire Smoke Inhalation, Inhalation Toxicology, 20, 761-766, 10.1080/08958370801975311, 2008.
Stier, P., Seinfeld, J. H., Kinne, S., Feichter, J., and Boucher, O.: Impact of nonabsorbing anthropogenic aerosols on clear-sky atmospheric absorption, Journal of Geophysical Research: Atmospheres, 111, n/a-n/a, 10.1029/2006JD007147, 2006.
Strawa, A. W., Elleman, R., Hallar, A. G., Covert, D., Ricci, K., Provencal, R., Owano, T. W., Jonsson, H. H., Schmid, B., Luu, A. P., Bokarius, K., and Andrews, E.: Comparison of in situ

aerosol extinction and scattering coefficient measurements made during the Aerosol Intensive Operating Period, Journal of Geophysical Research: Atmospheres, 111, n/a-n/a, 10.1029/2005JD006056, 2006.
Streets, D. G., Bond, T. C., Lee, T., and Jang, C.: On the future of carbonaceous aerosol emissions, Journal of Geophysical Research: Atmospheres, 109, n/a-n/a, 10.1029/2004JD004902, 2004.
Sumlin, B. J., Pandey, A., Walker, M. J., Pattison, R. S., Williams, B. J., and Chakrabarty, R. K.: Atmospheric Photooxidation Diminishes Light Absorption by Primary Brown Carbon Aerosol from Biomass Burning, Environmental Science & Technology Letters, 4, 540-545, 10.1021/acs.estlett.7b00393, 2017.
Sumlin, B. J., Heinson, Y. W., Shetty, N., Pandey, A., Pattison, R. S., Baker, S., Hao, W. M., and Chakrabarty, R. K.: UV–Vis–IR spectral complex refractive indices and optical properties of brown carbon aerosol from biomass burning, Journal of Quantitative Spectroscopy and Radiative Transfer, 206, 392-398, https://doi.org/10.1016/j.jqsrt.2017.12.009, 2018.
Sutherland, E. R., Make, B. J., Vedal, S., Zhang, L., Dutton, S. J., Murphy, J. R., and Silkoff, P. E.: Wildfire smoke and respiratory symptoms in patients with chronic obstructive pulmonary disease, Journal of Allergy and Clinical Immunology, 115, 420-422, 10.1016/j.jaci.2004.11.030, 2005.
Thompson, J. E., Smith, B. W., and Winefordner, J. D.: Monitoring Atmospheric Particulate Matter through Cavity Ring-Down Spectroscopy, Analytical Chemistry, 74, 1962-1967, 10.1021/ac0110505, 2002.
Thompson, J. E., Barta, N., Policarpio, D., and DuVall, R.: A fixed frequency aerosol albedometer, Opt. Express, 16, 2191-2205, 10.1364/OE.16.002191, 2008.
Tkacik, D. S., Robinson, E. S., Ahern, A., Saleh, R., Stockwell, C., Veres, P., Simpson, I. J., Meinardi, S., Blake, D. R., and Yokelson, R. J.: A Dual-Chamber Method for Quantifying the Effects of Atmospheric Perturbations on Secondary Organic Aerosol Formation from Biomass Burning Emissions: Investigation of Biomass Burning SOA, J. Geophys. Res. D: Atmos., 122, 6043, 2017.
Toole, J. R., Renbaum-Wolff, L., and Smith, G. D.: A Calibration Technique for Improving Refractive Index Retrieval from Aerosol Cavity Ring-Down Spectroscopy, Aerosol Science and Technology, 47, 955-965, 10.1080/02786826.2013.805875, 2013.
Uin, J., Tamm, E., and Mirme, A.: Very Long DMA for the Generation of the Calibration Aerosols in Particle Diameter Range up to 10 µm by Electrical Separation, Aerosol and Air Quality Research, 11, 531-538, 10.4209/aaqr.2011.05.0068, 2011.
UN: World Population Prospects: The 2010 Revision, Comprehensive Tables. ST/ESA/SER.A/313., United Nations, Department of Economic and Social Affairs, Population Division, 2011.
Vakkari, V., Beukes, J. P., Dal Maso, M., Aurela, M., Josipovic, M., and van Zyl, P. G.: Major Secondary Aerosol Formation in Southern African Open Biomass Burning Plumes, Nat. Geosci., 11, 580, 2018.
van der Werf, G. R., Randerson, J. T., Giglio, L., Collatz, G. J., Mu, M., Kasibhatla, P. S., Morton, D. C., DeFries, R. S., Jin, Y., and van Leeuwen, T. T.: Global fire emissions and the contribution of deforestation, savanna, forest, agricultural, and peat fires (1997–2009), Atmos. Chem. Phys., 10, 11707-11735, 10.5194/acp-10-11707-2010, 2010.

Wang, X., Liu, T., Bernard, F., Ding, X., Wen, S., Zhang, Y., Zhang, Z., He, Q., Lü, S., Chen, J., Saunders, S., and Yu, J.: Design and characterization of a smog chamber for studying gas-phase chemical mechanisms and aerosol formation, Atmos. Meas. Tech., 7, 301-313, 10.5194/amt-7-301-2014, 2014.

Ward, D. E., Susott, R. A., Kauffman, J. B., Babbitt, R. E., Cummings, D. L., Dias, B., Holben, B. N., Kaufman, Y. J., Rasmussen, R. A., and Setzer, A. W.: Smoke and fire characteristics for cerrado and deforestation burns in Brazil: BASE-B Experiment, Journal of Geophysical Research: Atmospheres, 97, 14601-14619, 10.1029/92jd01218, 1992.

Weingartner, E., Saathoff, H., Schnaiter, M., Streit, N., Bitnar, B., and Baltensperger, U.: Absorption of light by soot particles: Determination of the absorption coefficient by means of aethalometers, Journal of Aerosol Science, 34, 1445-1463, 10.1016/s0021-8502(03)00359-8, 2003.

Williams, J. E., Weele, M. v., Velthoven, P. F. J. v., Scheele, M. P., Liousse, C., and Werf, G. R. v. d.: The Impact of Uncertainties in African Biomass Burning Emission Estimates on Modeling Global Air Quality, Long Range Transport and Tropospheric Chemical Lifetimes, Atmosphere, 3, 132, 2012.

Yang, M., Howell, S. G., Zhuang, J., and Huebert, B. J.: Attribution of aerosol light absorption to black carbon, brown carbon, and dust in China – interpretations of atmospheric measurements during EAST-AIRE, Atmos. Chem. Phys., 9, 2035-2050, 10.5194/acp-9-2035-2009, 2009.

Yokelson, R. J., Crounse, J. D., DeCarlo, P. F., Karl, T., Urbanski, S., Atlas, E., Campos, T., Shinozuka, Y., Kapustin, V., Clarke, A. D., Weinheimer, A., Knapp, D. J., Montzka, D. D., Holloway, J., Weibring, P., Flocke, F., Zheng, W., Toohey, D., Wennberg, P. O., Wiedinmyer, C., Mauldin, L., Fried, A., Richter, D., Walega, J., Jimenez, J. L., Adachi, K., Buseck, P. R., Hall, S. R., and Shetter, R.: Emissions from biomass burning in the Yucatan, Atmos. Chem. Phys., 9, 5785-5812, 10.5194/acp-9-5785-2009, 2009.

Yokelson, R. J., Burling, I. R., Gilman, J. B., Warneke, C., Stockwell, C. E., de Gouw, J., Akagi, S. K., Urbanski, S. P., Veres, P., Roberts, J. M., Kuster, W. C., Reardon, J., Griffith, D. W. T., Johnson, T. J., Hosseini, S., Miller, J. W., Cocker Iii, D. R., Jung, H., and Weise, D. R.: Coupling field and laboratory measurements to estimate the emission factors of identified and unidentified trace gases for prescribed fires, Atmos. Chem. Phys., 13, 89-116, 10.5194/acp-13-89-2013, 2013.

Zhang, H., Hu, D., Chen, J., Ye, X., Wang, S. X., Hao, J. M., Wang, L., Zhang, R., and An, Z.: Particle Size Distribution and Polycyclic Aromatic Hydrocarbons Emissions from Agricultural Crop Residue Burning, Environmental Science & Technology, 45, 5477-5482, 10.1021/es1037904, 2011.

Page 8: [1] Deleted **damonmsmith87@gmail.com** **4/17/20 3:56:00 PM**

To represent a polluted urban environment, we used emission inventory for urban environments from South Africa. This does not necessarily represent the east African emission inventory but this serves as a proxy since this is the only available data to us for the continent. This was obtained from South African Air Quality Information System (SAAQIS). NOx, NO, NO_2, CO, O_3, benzene, toluene, xylene, and ethylbenzene data for several South African Sites (Diepkloof, Kliprivier, Three Rivers, Sharpeville, Zamdela, Thabazimbi, Lephalale, Phalaborwa, and Mokopane) were obtained.

The VOC data was obtained from the two weeks (M-F) of July 11 – 15 and July 18 – 22. These two weeks were in the middle of the peak burning season for South Africa for the year 2016. For the urban area, a ratio of 5:14:6 by concentration (in ppm) for benzene, toluene, and xylene, respectively were used. These concentrations were converted into mass using the volume of the chamber (9010 L), the normal temperature of the chamber (296.64 K), and the normal pressure of the chamber (0.9728 atm). Using the molecular weights of benzene (78.11 g mol^{-1}), toluene (92.14 g mol^{-1}), and xylene (106.17 g mol^{-1}), masses of 0.1406 mg, 0.4645 mg, and 0.8345 mg, respectively were calculated. This was converted into a volume, leading to 0.36 µL for each species, making them equivalent by volume. A mixture was prepared using equal amounts (by volume) of benzene, toluene, and xylene, and was injected by syringe into the U-shaped tube attached to the chamber. This tube was then flushed by zero air into the chamber. The concentration injected into the chamber was approximately 12 times more concentrated than the values found from the emissions data. This was mostly due to ease of sample preparation since the amounts needed for an exact match were too small for our scale to weigh appropriately.

Table 1. Average concentrations (in ppm) of urban emissions for the two weeks of July 11 – 15 and July 18 – 22, 2018. Source South African Air Quality Information System (SAAQIS) The urban summary was used to create a solution of VOCs for use in the smog chamber. Concentrations in the chamber are intentionally higher than atmospheric conditions, to age the BB aerosol faster.

	Urban Summary			**Suburban Summary**			
Diepkloof	Benzene	Toluene	Xylene	**Sebokeng**	Benzene	Toluene	Xylene
Average	1.09	3.95	1.12	Average	2.976	7.874	0.26
Rounded	1	4	1	Rounded	3	8	0.25
Kliprivier	Benzene	Toluene	Xylene	**Three Rivers**	Benzene	Toluene	Xylene
Average	1.23	3.01	1.76	Average	0.698	1.914	0.57
Rounded	1.25	3	1.75	Rounded	0.75	2	0.5
Combined	Benzene	Toluene	Xylene	**Zamdela**	Benzene	Toluene	Xylene
Averaged	1.16	3.48	1.44	Average	1.382	2.283	1.282
Rounded	1.25	3.5	1.5	Rounded	1.5	2.25	1.25
Ratio	5	14	6				
				Combined	Benzene	Toluene	Xylene
				Averaged	1.69	4.02	0.7
				Rounded	1.75	4	0.75
				Ratio	7	16	3

Page 10: [2] Deleted **Microsoft Office User** **4/27/20 2:04:00 PM**

measurements from will be more impact by multiply charged particles those from the

[RP1]

Page 14: [3] Deleted	damonmsmith87@gmail.com	4/17/20 10:10:00 PM

The measured SSA values for 800° C combustions were below 0.5, which indicates highly absorbing aerosol and corresponds to aerosol dominated by black carbon (Pokhrel et al., 2016). The calculated MCE (average from 12 different burns 0.974 ± 0.015) also supports the fact that aerosol emitted from combustion at 800° C represents the flaming stage, which is dominated by BC. The flaming stage of combustion produces more black carbon and less organic carbon which explains the lower values of SSA at visible wavelengths. The impact of combustion temperature on aerosol can be separated visually by looking at the color of the collected filter samples as shown in Fig. S1. As evident from Fig. S1, aerosol emitted from the 800° C combustion looks black whereas that from 500° C combustion looks brownish, indicating a visual difference between black and brown carbon emitted from same fuel under different combustion temperatures. Under the same combustion conditions and airflow, there is a clear but small dependence of SSA on fuel type with eucalyptus producing aerosol with higher SSA than olive and acacia.

While variations in SSA between fuels under similar combustion temperature is relatively small, we observed a large increase in the SSA for samples combusted at 500° C. The range of SSA between different fuels combusted at 800° C is (0.287 to 0.439), whereas the range for of the same fuels combusted at 500° C is (0.66 to 0.769). This indicates that aerosol emissions are dominated by more scattering particles at the lower combustion temperature. This fact is also supported by lower MCE values (averaged from four different burns 0.878 ± 0.008) when combusted at 500° C, where the aerosol is dominated by organic carbon (Christian et al., 2003a;Ward et al., 1992). This is consistent with the finding that low temperature biomass burning results in the formation of primary BrC (Bahadur et al., 2012;Lewis et al., 2008;Radney et al., 2017). Like combustion at 800° C, the SSA depends on fuel type, which might be due to the difference in the chemical compositions of the emitted aerosol. The range of SSA for combustion at 500° C is comparable to previous studies with similar MCE (Liu et al., 2014;Pokhrel et al., 2016). On comparing the SSA of the three different fuels under two different combustion temperatures, it is apparent that SSA is controlled more by the combustion conditions rather than the fuel types. There is a larger variation in SSA for the same fuel under two different combustion conditions compared to the variation due to the inter fuel variability under the same combustion temperature. This result is consistent with the previous study, which showed that SSA is highly correlated with the EC/TC (proxy for the combustion conditions), even for a wide variety of fuels (Pokhrel et al., 2016). A complete list of size-selected SSA of different fuels measured at two combustion temperatures and under different aging conditions is provided in Table S1.

Page 15: [4] Deleted	Microsoft Office User	4/18/20 8:11:00 AM

Page 17: [5] Deleted	Microsoft Office User	4/27/20 2:18:00 PM

Nighttime chemistry in BB studies is still unclear (Hodshire et al., 2019). The potential mechanism for the observed result could be due to nighttime oxidation initiated by ozone or nitrate chemistry or the formation of less/non-absorbing secondary organic aerosol. To further explore the possibility of the observed increase in SSA, we looked at the scattering and extinction cross-section of the fresh and dark aged aerosol. Figure S2 shows the changes in

extinction and scattering cross-section of 300 nm size particles emitted during combustion at 500^{o} Csmoldering dominated combustion under dark aging. For all fuel types studied, there occurred a significant increase in the scattering and extinction cross-section, indicating the occurrence of chemistry, even during dark aging. The increase in cross-section was driven by the scattering cross-section, with no significant change in absorption cross-section during aging. This fact cannot be explained by the heterogeneous chemistry[MNF2] in aerosol phase when the particle size is selected, because one expects a decrease in absorption cross-section if scattering cross-section of the particle increases. Heterogeneous chemistry is common at high relative humidity (Shi et al., 2014). We hypothesized secondary organic aerosol formation as a potential phenomenon happening during dark aging. It was observed that dark aging produced higher amounts of nitrogen containing organic compounds in the aerosol phase (Li et al., 2015;Ramasamy et al., 2019;Hartikainen et al., 2018) which could be a possible explanation for our experimental results. The fact that the production of non-absorbing secondary organic aerosol will increase the scattering cross-section of the particles without altering the absorption cross-section explains the observed behaviors in our experiments.

Page 22: [6] Deleted **Microsoft Office User** **4/27/20 2:28:00 PM**

Biomass burning is the major source of atmospheric primary particles and vapors, which are precursors for secondary aerosols. BB aerosols have been extensively studied through both field and laboratory environments for North American fuels to understand the changes in optical and chemical properties as a function of aging. There is a clear research need for a wider sampling of fuels from different regions of the world for laboratory studies. This work is such an attempt to study the optical and chemical properties of fuels common in east Africa and represents the first such study.

The existence of significant variability in the observed field and laboratory measurements has been reviewed recently (Hodshire et al., 2019). While laboratory studies provide control over environmental and chemical conditions to study aging by controlling one variable at a time, it may not necessarily recreate atmospheric conditions in atmospheric plumes in the field. Differences in fuel mixture and fuel conditions, such as moisture content, can lead to different emissions. There is a difference in dilution rates between field studies, which is variable, and laboratory studies, which are not variable. Other differences include temperature differences, and background OA concentrations, and wall losses. Despite the gap in reconciling field and laboratory studies, some limited comparisons can be made.

For fresh emissions, SSA showed no pronounced size dependence for flaming dominated combustion at 800^{o} C, whereas some size dependence was observed for smoldering dominated combustion at 500^{o} C, some size dependence was observed. This may be due to the impact of multiply charged aerosol, which is not discriminated by the DMA. For the wavelength range used in this study, no wavelength dependence of SSA was observed under all conditions. However, SSA shows dependence on fuel type in general, even under the same combustion conditions.

In general, combustion temperature plays a major role in the optical properties of the emitted aerosol. In all cases the measured SSA values for flaming dominated combustion at 800^{o} C are in the range between 0.287 and 0.439, indicating highly absorbing aerosol, which corresponds to aerosol dominated by black carbon. We observed a large increase in the SSA during smoldering dominated combustion at 500^{o} C, which is in the range between 0.66 and 0.769. Under the same combustion conditions and airflow, there is a clear dependence of SSA on fuel type, with eucalyptus

producing aerosol with higher SSA values than olive and acacia. However, these variations are relatively small, indicating that the SSA is more controlled by the combustion conditions than the fuel types[MNF3].

Negative mode UPLC/DAD-ESI-HR-QTOFMS analyses of fresh BBA from flaming-dominated combustion suggest that there is some chemical constituent that is not being captured by this analysis. Given that Eucalyptus has a higher SSA than Acacia, this would indicate that Eucalyptus has more non-absorbing OA that is not observed by chemical analysis, such as the presence of eucalyptol. Smoldering-dominate combustion of Eucalyptus and Acacia produced a variety of compounds in common, such as lignin pyrolysis products, distillation products, and cellulose breakdown products. Several lignin pyrolysis products and distillation products are more prevalent in Eucalyptus than in Acacia, while pyrolysis products of cellulose and at least one nitroaromatic species were more prevalent in Acacia. This is consistent with the higher SSA of Acacia when compared to Eucalyptus, since lignin pyrolysis products and distillation products are known chromophores, while compounds derived from sugars and cellulose are non-chromophores.

Regardless of fuel types, there occurred an increase in SSA during dark aging, with some fuel dependence, the largest of which was observed for smoldering dominated aerosol emitted from olive combusted at 500^{o} C. A significant increase in the scattering and extinction cross-section (mostly dominated by scattering) was observed, indicating the occurrence of chemistry, even during dark aging. This fact cannot be explained by the heterogeneous chemistry and we hypothesized that secondary organic aerosol formation as ais potentially phenomenon happoccurring during dark aging. This is also consistent with previous work thatthe [MNF4]observed production of nitrogen containing organic compounds during dark aging.[MNF5] The fact that the production of non-absorbing secondary organic aerosol will increase the scattering cross-section of the particles without altering the absorption cross-section explains the observed behaviors in our experiments.

After 12 hours of photochemical aging, BB aerosol becomes highly scattering with SSA values above 0.9, even though fresh emissions were more absorbing with SSA below 0.8. This can be attributed to oxidation in the chamber.

Due to the very low number concertation of flaming dominated aerosols during aging studies of combustion at 800° C, the results were inconclusive, and we plan to conduct measurements by increasing the amount of fuel burned. We also attempted to simulate polluted urban environments by injecting anthropogenic VOCs into the chamber, but no distinct difference was observed, since measurements were done 12 hours after injection of VOCs. An examination of the chemical composition of aged BBA shows very few species that could be attributed to anthropogenic VOCs. Generally, very few compounds were produced to a significant extent, and both fuels were dominated by a loss of chromatophoric lignin pyrolysis and distillation products, likely caused by a combination of photo-bleaching, heterogeneous OH oxidation, and SOA formation of non-chromophores. No significant OA enhancement was observed because of the VOC injection either, even though significantly enhanced SOA formation was observed in polluted environments.[MNF6] This suggests a need for more rigorous controlled time dependent measurements.

To our knowledge, this is the first laboratory study of optical properties of east African biomass fuels for domestic use. Ongoing work includes systematic study of optical properties using six different African fuels as a function of aging, burn conditions, VOC concenrtration, and RH